Genetic Architecture of Flowering-Time Variation in Arabidopsis thaliana

DOI: 10.1534/genetics.111.126607

Genetic Architecture of Flowering-Time Variation in *Arabidopsis thaliana*

Patrice A. Salomé,* Kirsten Bomblies,*,[1] Roosa A. E. Laitinen,* Levi Yant,*,[1] Richard Mott† and Detlef Weigel*,[2]

**Department of Molecular Biology, Max Planck Institute for Developmental Biology, D-72076 Tübingen, Germany and* †*Wellcome Trust Centre for Human Genetics, University of Oxford, Oxford OX3 7BN, United Kingdom*

Manuscript received January 15, 2011
Accepted for publication March 9, 2011

ABSTRACT

The onset of flowering is an important adaptive trait in plants. The small ephemeral species *Arabidopsis thaliana* grows under a wide range of temperature and day-length conditions across much of the Northern hemisphere, and a number of flowering-time loci that vary between different accessions have been identified before. However, only few studies have addressed the species-wide genetic architecture of flowering-time control. We have taken advantage of a set of 18 distinct accessions that present much of the common genetic diversity of *A. thaliana* and mapped quantitative trait loci (QTL) for flowering time in 17 F_2 populations derived from these parents. We found that the majority of flowering-time QTL cluster in as few as five genomic regions, which include the locations of the entire *FLC/MAF* clade of transcription factor genes. By comparing effects across shared parents, we conclude that in several cases there might be an allelic series caused by rare alleles. While this finding parallels results obtained for maize, in contrast to maize much of the variation in flowering time in *A. thaliana* appears to be due to large-effect alleles.

THE correct timing of flower initiation is critical for a variety of reasons. For example, depending on geography, the season during which a plant can successfully complete seed set is more or less limited. Similarly, in outcrossing species, synchronized flowering of conspecifics ensures that pollen can be exchanged, a prerequisite for fertilization. Research aimed at understanding the multiple layers of control in floral initiation has been a very active field over the past 40 years and has followed several complementary directions. First, forward and reverse genetics, primarily in *Arabidopsis thaliana* and rice, have led to the identification of many genes that promote or repress flowering. These so-called flowering-time genes have since been placed in a number of genetically defined pathways that integrate external stimuli such as photoperiod, ambient temperature, or prolonged exposure to cold, with endogenous signals including phytohormones and plant age (Bäurle and Dean 2006; Kobayashi and Weigel 2007; Turck *et al.* 2008; Greenup *et al.* 2009; Amasino 2010).

In parallel, *A. thaliana* has emerged as a powerful platform from which to study the genetic basis of naturally occurring variation in flowering time. *A. thaliana* accessions are found across much of the Northern hemisphere and grow under local conditions for which many have presumably become adapted. Usually starting with the mapping of quantitative trait loci (QTL) in crosses derived from two parents, the analysis of naturally occurring alleles has confirmed the importance of several proteins in the control of flowering, among them the photoreceptors CRYPTOCHROME2 (CRY2), PHYTOCHROME B (PHYB), and PHYC (El-Din El-Assal *et al.* 2001; Balasubramanian *et al.* 2006; Filiault *et al.* 2008), HUA2, a likely pre-mRNA processing factor (Wang *et al.* 2007), the mobile flowering signal FT (Schwartz *et al.* 2009), and the MADS domain transcription factor FLOWERING LOCUS M (FLM)/MADS AFFECTING FLOWERING 1 (MAF1) (Werner *et al.* 2005). FLM belongs to a small clade of transcription factors that comprises FLC and the four closely related MAF proteins, MAF2 to MAF5, encoded in a tandem cluster (Ratcliffe *et al.* 2001; Ratcliffe *et al.* 2003; Scortecci *et al.* 2003). This cluster is polymorphic between accessions and has recently been implicated in natural variation of flowering as well (Caicedo *et al.* 2009; Rosloski *et al.* 2010).

In addition to these factors, which had been identified already as actual or potential regulators of flowering through forward or reverse genetics studies, the role of FLC and its regulator FRIGIDA (FRI) was revealed only through the analysis of natural accessions, as they are defective in several of the early flowering accessions used commonly for laboratory studies (Michaels and

Supporting information is available online at http://www.genetics.org/cgi/content/full/genetics.111.126607/DC1.

[1]*Present address:* Department of Organismic and Evolutionary Biology, Harvard University, 22 Divinity Ave., Cambridge, MA 02138.

[2]*Corresponding author:* Department of Molecular Biology, MPI for Developmental Biology, Spemannstrasse 37-39, D-72076 Tübingen, Germany. E-mail: weigel@weigelworld.org

TABLE 1

The 17 Arabidopsis F_2 populations generated in this study

Population	Grandmother	Origin[b]	Grandfather	Origin[b]
P35	Tamm-2	Finland	Col-0	(Poland)
P66	Fei-0	Portugal	Col-0	(Poland)
P145	Sha	Tajikistan	Fei-0	Portugal
P2	Lov-5	Sweden	Sha	Tajikistan
P19	Bay-0	Germany	Lov-5	Sweden
P3	Bur-0	Ireland	Bay-0	Germany
P10	Bur-0	Ireland	Cvi-0	Cape Verde Islands
P17	Cvi-0	Cape Verde Islands	RRS7	United States
P8	Est-1	Estonia	RRS7	United States
P12	Est-1	Estonia	Br-0	Czech Republic
P15	Br-0	Czech Republic	C24	(Portugal)
P129	C24	(Portugal)	RRS10	United States
P9	Tsu-1	Japan	RRS10	United States
P169	Ts-1	Spain	Tsu-1	Japan
P6[a]	Van-0	Canada	Bor-4	Czech Republic
P7[a]	NFA-8	United Kingdom	Van-0	Canada
P20[a]	Bor-4	Czech Republic	NFA-8	United Kingdom

[a]Triangular crossing design.
[b]Parentheses indicate uncertainty of precise geographic origin.

Amasino 1999; Sheldon *et al.* 1999; Johanson *et al.* 2000). It has been estimated that the *FLC* and *FRI* loci account for almost three-quarters of the flowering-time variation among accessions, when these are not exposed to several weeks of winter-like conditions, known as vernalization. Upon vernalization, the contribution of *FLC* and *FRI* becomes markedly reduced (Lempe *et al.* 2005; Shindo *et al.* 2005). Notably, the variant alleles identified at *CRY2*, *FLM*, *FT*, *HUA2*, and *PHYB* are all rare, and it is therefore unclear how much these genes contribute to the global genetic architecture of flowering-time control in *A. thaliana*, although functionally distinct *PHYC* and *MAF2-5* alleles appear to be quite common (Balasubramanian *et al.* 2006; Caicedo *et al.* 2009).

An alternative to genetic mapping is the use of genome-wide association studies (GWAS) to identify common variants controlling a trait, and this approach has recently been implemented in *A. thaliana* (Atwell *et al.* 2010; Brachi *et al.* 2010). Unfortunately, the analysis of flowering time by GWAS is strongly confounded by population structure, and even the re-identification of *FLC* and *FRI* was not straightforward, although this might change in the future with larger populations, or more appropriately chosen collections of accessions. Furthermore, there was essentially no overlap with genes identified in QTL studies.

Here, we took advantage of a set of 18 distinct accessions that present much of the common genetic diversity of *A. thaliana* (Clark *et al.* 2007). We generated 17 F_2 populations and phenotyped almost 500 plants of each population in a common environment. An integrated analysis of this data set was greatly facilitated by all plants being genotyped with the same intermediate-frequency SNPs chosen to be maximally informative across the 17 populations. The detailed picture of the genetic architecture of flowering-time variation in these F_2 populations validates and extends previous studies focused on recombinant inbred lines (RILs), by identifying QTL clusters that have not been described before. Much of the mappable variation in flowering time can be attributed to as few as five genomic regions, mirroring the results of a recent study with a similar design, but growing plants in a variable environment (Brachi *et al.* 2010). The regions we identified include the locations of the entire *FLC/MAF* clade of transcription factor genes. By comparing effects across shared parents, we conclude that in several cases there might be an allelic series, which parallels results obtained for maize (Buckler *et al.* 2009). In contrast to the many but small- to modest-effect QTL in maize, however, much of the variation in flowering time in *A. thaliana* appears to be due to large-effect alleles.

MATERIALS AND METHODS

Plants and growth conditions: Seeds of 18 accessions were from the individuals described by Clark and Colleagues (2007). All accessions were crossed to each other in a full diallel. Out of the 306 F_1 crosses, 14 were chosen in a simple round-robin design, such that 13 parents were represented twice and two parents once. Three additional crosses represented a triangular design with three parents. The list of parental accessions and the crossing design are provided in Table 1 and supporting information, Figure S1.

Parents and F_1 and F_2 progeny were grown under identical conditions. Seeds were stratified in 0.1% top agar for 4 days in the dark at 4°, before being sown on soil. Seeds were first allowed to break dormancy at 16° overnight, before being subjected to 6 weeks vernalization at 4° under 8-hr photoperiods (short days), to reduce differences in flowering time.

Upon release from vernalization, all seeds had germinated, and cotyledons were expanded. A single seedling was kept in each pot and allowed to grow in 16-hr-long days, at a constant temperature of 16°. Trays were rotated 180° and moved to a new shelf every other day to minimize position effects within the growth chamber. Humidity inside the chamber was maintained at 65%, and lights were provided with a combination of cool white and warm white fluorescent lights, for a fluence of 125 to 175 μmol m^{-2} s^{-1}.

For F_1 plants and parental accessions, 8 pots were sown for each genotype in a randomized fashion across two 40-pot trays. F_2 seeds were sown in 12 40-pot trays, for a total of 480 plants. Because of lack of germination in some pots, the number of F_2 plants per population varied between 239 and 462. The 17 populations were analyzed in four overlapping cohorts, grown from July 2007 to January 2008: P2 and P3 (cohort 1); P6, P7, P8, P9, and P10 (cohort 2), P12, P15, P17, P19, and P20 (cohort 3); P35, P66, P129, P145, and P169 (cohort 4). F_1 plants and parental accessions were grown immediately following cohort 4, in January and February 2008.

The 96 Nordborg (Nordborg *et al.* 2005) accessions were grown last in cohort 5; 10 pots per accession were sown. Accessions were divided into two sets of 48, and sown in 12 40-pot trays in a randomized fashion. After 4 weeks of growth at 16°, pots from each accession were grouped together, to decrease shading of smaller accessions.

Phenotyping: Flowering time, number of rosette, and number of cauline leaves were recorded. Flowering time was first assessed when floral buds became visible in the center of the rosette (DTF1), when the main shoot had elongated to 1 cm (DTF2), and last when the first flower opened (DTF3). The number of rosette leaves was also recorded at DTF2, and the number of cauline leaves was counted 1–2 weeks later. A complete list of traits measured is listed in Table S1.

Genotyping: A single leaf from each F_2 plant and parental accession was collected after plants had flowered and used for DNA extraction using the BioSprint 96 workstation (Qiagen, Hilden, Germany). Quality of genomic DNA was tested on an agarose gel; DNA concentrations were determined on a Nanodrop photometer (Thermo Scientific, Waltham, MA). About 2 μg of genomic DNA was used for genotyping of SNP markers by Sequenom (San Diego, CA), using MassArray technology (Jurinke *et al.* 2001). Genotypes are available in File S2.

QTL mapping: Raw genotype data were converted to the appropriate genotype format A, B, H (A being a marker homozygous for parent A; B homozygous for parent B; H a heterozygous marker). Genotype and phenotype data were merged and saved as .csv files. QTL analysis was performed using R/qtl, with simple and composite interval mapping (Broman *et al.* 2003). The confidence intervals around each significant QTL peak were determined with the *baysint* function, at 95% confidence levels. Additional information on the extent of variation explained by each QTL, as well as the effect associated with each parental allele, was gathered using the *sim.geno*, *makeqtl*, *fitqtl*, *effectplot,* and *effectscan* functions. Epistatic interactions between QTL were identified by using the *qb.scantwo* function in R/qtlbim (Yandell *et al.* 2007).

For joint QTL analysis, all F_2 plants were combined into a single population, the genotype of each chromosome at any given SNP taking on 1 of the 18 possible identities (from our founding accessions). Evidence for a QTL is given as log *P*, *P* being the probability that a QTL is segregating at a given SNP (Kover *et al.* 2009).

QTL data on flowering time obtained from RIL analysis were taken from published studies (Alonso-Blanco *et al.* 1998; Loudet *et al.* 2002; Weinig *et al.* 2002; El-Lithy *et al.* 2004, 2006; Werner *et al.* 2005; O'neill *et al.* 2008; Simon *et al.* 2008).

RESULTS

Variation in flowering time among 17 F_2 populations: We measured flowering time for 7045 F_2 plants, as well as 136 F_1 plants and 128 plants from the 18 parental accessions in 5 cohorts as described in materials and methods. A final cohort consisted of 960 plants from a larger group of 96 *A. thaliana* accessions, chosen over the geographical range of the species and representative of its phenotypic and genetic diversity (Nordborg *et al.* 2005). Previous studies have found strong correlations between days until flowering and the number of rosette leaves produced on the main shoot (Alonso-Blanco *et al.* 1998; El-Din El-Assal *et al.* 2001; Lempe *et al.* 2005; El-Lithy *et al.* 2006; Simon *et al.* 2008), indicating that these two traits are genetically linked in natural accessions. Under our conditions, we observed a similar positive linear relationship between days to flower and leaf number for the parental accessions ($r^2 = 0.88$; see Figure 1A). When we excluded Cvi-0, which grew very slowly, correlation was even higher ($r^2 = 0.96$), similar to what we found with the 96 Nordborg (Nordborg *et al.* 2005) accessions ($r^2 = 0.98$; Figure S2). The slopes of the regression line between days to flower and leaf number from the founding accessions and the larger set of 96 accessions were close to parallel (the regression coefficient being 0.97 for founding accessions, 0.88 for the full set of 96 accessions, or 0.93 when the latest flowering accessions are excluded).

In contrast, the correlation between days to flower and leaf number in F_2 populations dramatically decreased, with a maximum of $r^2 = 0.84$ for P9 (Tsu-1 × RRS10). In several instances the correlation was only marginal, as in the P6 (Van-0 × Bor-4: $r^2 = 0.3$), P8 (Est-1 × RRS7: $r^2 = 0.28$), and P66 populations (Fei-0 × Col-0: $r^2 = 0.26$, Figure 1A); this suggests that days to flower and leaf number are canalized in natural accessions, but that the link between the two can be genetically uncoupled. This observation can only partially be explained by the smaller spread of flowering times in each population (Figure 1B). While in most F_2 populations r^2 values tended to increase with increased variance in flowering time, P12 (Est-1 × Br-0), P15 (Br-0 × C24), P66 (Fei-0 × Col-0), and P129 (C24 × RRS10) formed a distinct group (left-side circle, Figure 1B) with small variances, but differing r^2 values. In some populations (for example, NFA-8 × Van-0 [P7], Bor-4 × NFA-8 [P20], Sha × Fei-0 [P145], and Ts-1 × Tsu-1 [P169]), a small group of plants appeared to initiate leaves at a slower rate than their siblings (Figure 1A), which might reflect variation in growth rate. Finally, the range in flowering time measured within each F_2 population did not correlate with differences in flowering time between the parental accessions (Figure 1C), reflecting rampant transgressive segregation, which was evident in all populations, even though the founding grandparents had not been selected for differences in flowering

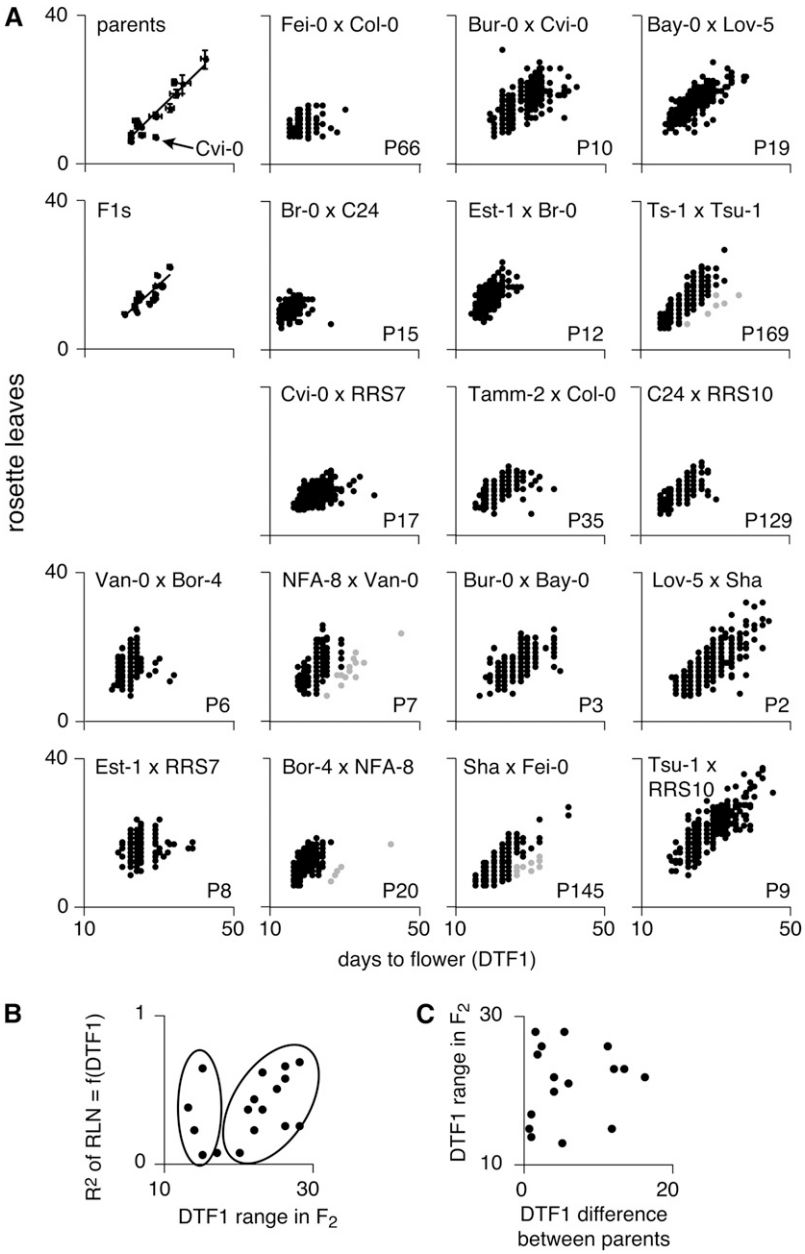

FIGURE 1.—Flowering-time variation in parental accessions, F_1 and F_2 populations. (A) Correlation between rosette leaf number and days to flower. F_2 populations are sorted in order of increasing r^2 values. Seedlings with lower leaf initiation rate in the NFA-8 × Van-0 (P7), Bor-4 × NFA-8 (P20), Sha × Fei-0 (P145), and Ts-1 × Tsu-1 (P169) populations are shown as gray dots. (B) Correlation between the r^2 values for rosette leaf number and days to flower and flowering-time variance in F_2 populations. (C) Flowering-time variance in F_2 populations is independent of the phenotypic differences of grandparents.

time. In fact, 8 of the 17 pairs of grandparents showed no significant differences in their flowering time in our conditions (Figure 2).

QTL for flowering time: All 7045 F_2 plants were genotyped with a common set of SNP markers, with 215 to 257 markers (mean 237) being informative in each population (P. SALOMÉ and D. WEIGEL, unpublished results). With an average of 400 plants per population, and a mean 237 informative SNPs, the amount of variance explained by a given QTL is very close to the LOD value for that QTL peak (File S1, Figure S3, and not shown). In essence, a QTL with a LOD score of 10 will explain 10% of the observed variation. With a significance threshold of LOD 3–4 for most populations, we therefore have the power to detect QTL with effects as small as 3–4% of the total variance. Population-wide scans revealed two to five flowering-time QTL per population, with an average of 3.2 and a total of 55 QTL (Figure 3, A and B, Table S2, and Table S3). The effects of all but one QTL exceeded 1 day, which is in stark contrast to only 7 of 333 in maize exceeding the 1-day threshold (Figure S4, BUCKLER *et al.* 2009). In the vast majority of populations, a single QTL per chromosome could be detected, indicating that measured effects at a given genomic location were not confounded by the local genetic background. When two QTL located to the same chromosome, they mapped to opposite arms and were therefore too distant from each other to influence their colocating QTL and associated effects (Table S2 and Table S3).

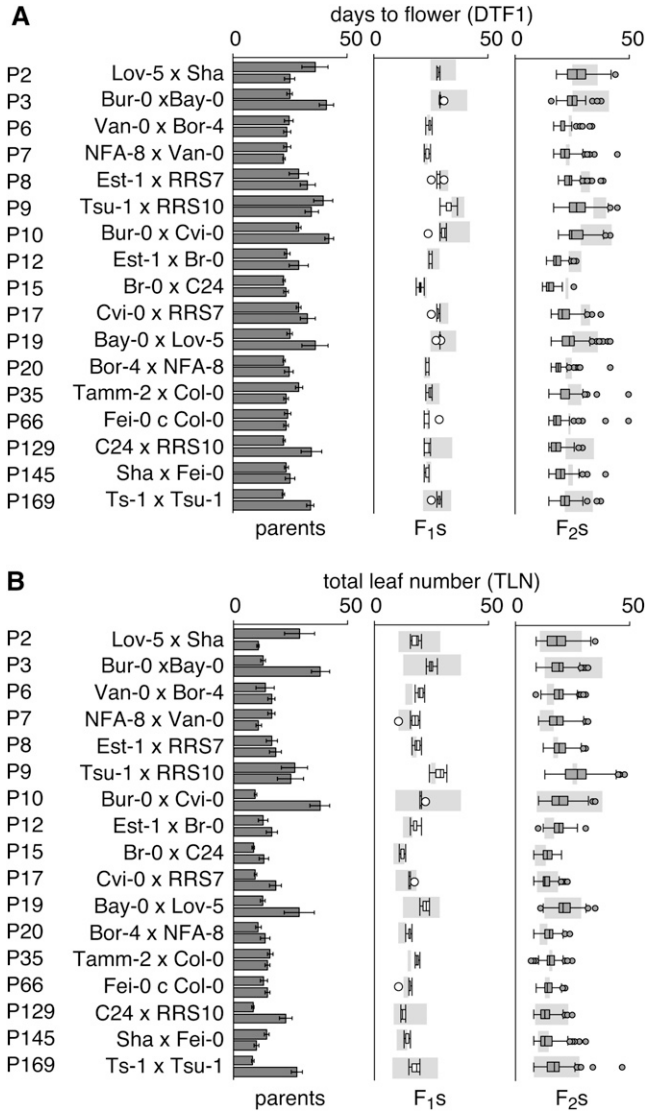

FIGURE 2.—Transgressive segregation of flowering time. Comparison of days to flower (A) and total leaf number (B) for parental accessions, F_1 hybrids, and all F_2 populations. Light blue bars indicate the parental difference in flowering time in the F_1 and F_2 columns.

Flowering-time-related traits (such as days to flower [DTF1, DTF2, and DTF3] and leaf number [rosette, cauline, and total leaf number]) were highly correlated and confidence intervals of QTL peaks for these traits usually overlapped in a given population. While variation in leaf initiation rate would provide the simplest explanation for a lack of correlation between days to flower and rosette leaf number, we detected leaf initiation rate QTL irrespective of the degree of correlation (Figure 3B). For the trait DTF1, number of days until the inflorescence first became visible to the unaided eye, QTL could explain between 10 and 64% (mean 39%) of the total phenotypic variation, with individual QTL accounting for 3–54% of variation (Table 2). The remainder is not due to rampant epistatic interactions between these QTL: we detected 11 strong epistatic pairs between QTL from 9 populations, but these accounted for only a mean of 1.6% of the total variance (range 0.35–3.3; see Table S4 and Figure S5).

Measured effects and prediction of parental flowering times: We extracted individual effects associated with parental alleles at each QTL and arranged the 17 F_2 populations on the basis of the sum of effects (Figure 4, A and B). Some populations displayed comparable positive and negative effects, which canceled each other out to give mean population values close to zero. Other populations were dominated by effects in a single direction. For example, the effects in Lov-5 × Sha (P2), Bur-0 × Bay-0 (P3), and Bur-0 × Cvi-0 (P10) were mostly negative, while those in Bay-0 × Lov-5 (P19), C24 × RRS10 (P129), and Ts-1 × Tsu-1 (P169) were largely positive (Figure 4, A and B). Although the detected QTL peaks accounted, on average, for 39% of the observed variation in flowering time, the measured cumulated effects could predict well the differences in flowering time between parental accessions (Figure 4, A and B).

Comparative power of QTL detection in F_2 and RIL populations: We compared the power of QTL detection reported in RILs (ALONSO-BLANCO *et al.* 1998; LOUDET *et al.* 2002; WEINIG *et al.* 2002; EL-LITHY *et al.* 2004, 2006; WERNER *et al.* 2005; O'NEILL *et al.* 2008; SIMON *et al.* 2008) with our F_2 populations. Only small-effect QTL, explaining <3% of variance, were more frequently reported in RIL studies. Since much of the variation is due to large-effect QTL, the total variance explained in our F_2 populations is not greatly different than that in RIL populations (Figure 5A). Effects measured in our study for specific QTL such as *FRI* and *FLC* are comparable to those reported in RIL studies (Figure 5B; and see below).

Common flowering-time QTL and the FLC clade: Since we measured flowering time in 17 large populations under the same conditions, we were in a good position to assess the contribution of genomic regions identified by QTL mapping to the global control of flowering time in the species. Simple interval mapping (IM) and composite interval mapping (CIM) identified the same QTL peaks (Figure S6). As many as 39 of the 55 detected QTL overlapped across populations, suggesting that distinct alleles segregate among accessions (Figure 3B, Table 2, and Table S2). Flowering-time QTL were overrepresented in four genomic regions, on chromosomes 1, 4, and 5. A joint analysis across all 17 F_2 populations identified in addition to the same four regions only the middle of chromosome 2 as making a small but significant contribution to flowering-time variation (Figure 3C), thus confirming the importance of these four regions in shaping the genetic architecture responsible for the measured variation in flowering time.

Major contributors to flowering-time variation in our populations include QTL that map to three genomic

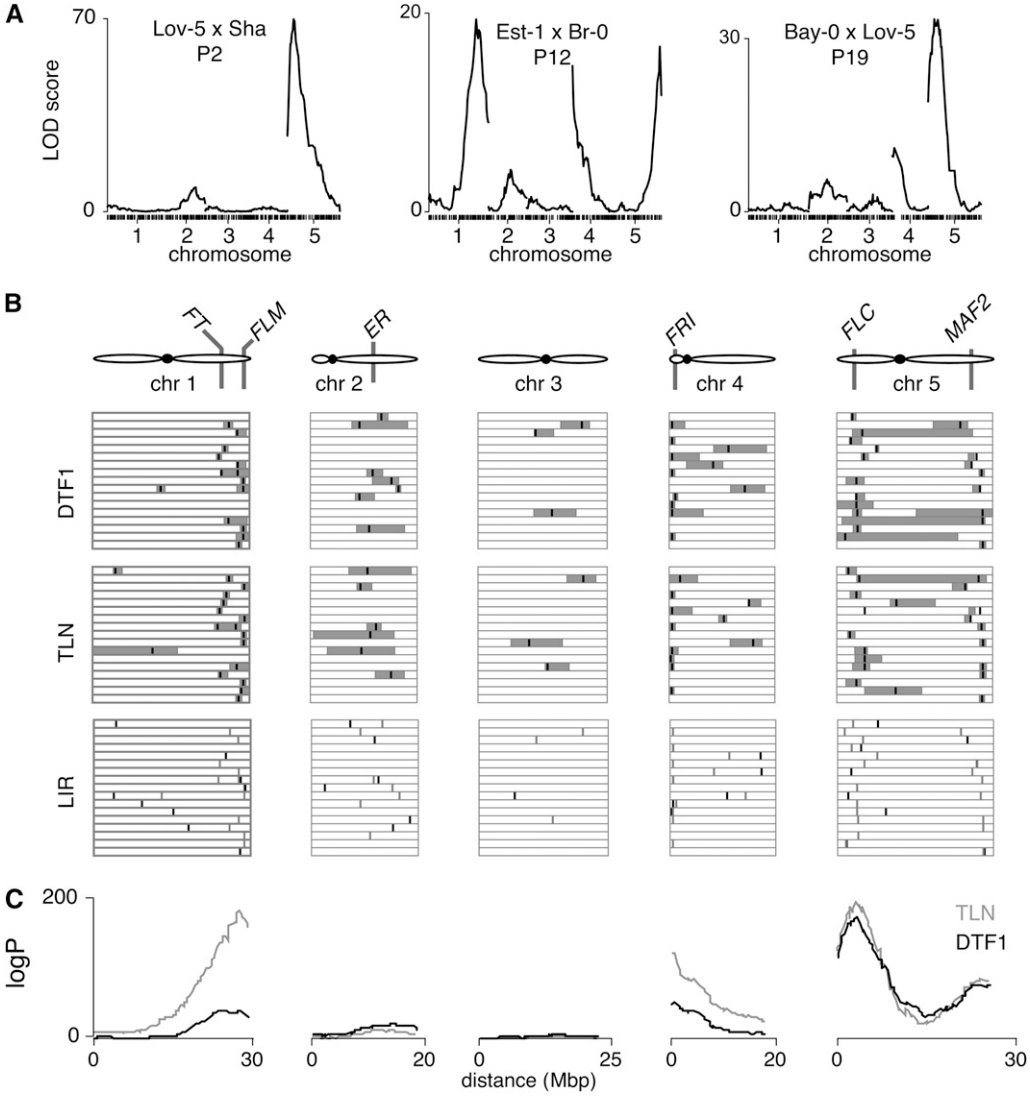

FIGURE 3.—Location of flowering-time QTL. (A) Examples of QTL maps for DTF1 in three distinct F_2 populations from simple interval mapping. (B) Location of QTL for days to flower (DTF1), total leaf number (TLN), and leaf initiation rate (LIR) in all 17 F_2 populations. The positions of al DTF1 QTL are shown in gray in the LIR row. (C) Joint QTL analysis, across all 17 F_2 populations.

regions containing members of the *FLC/MAF* clade of transcription factors. Without vernalization, *FLC* and its activator *FRI* can explain over 70% of the total flowering-time variation between wild accessions (LEMPE *et al.* 2005; SHINDO *et al.* 2005). QTL associated with the genomic regions containing members of the *FLC* clade (*FLM*, on the bottom of chromosome 1; *FLC*, on the top of chromosome 5; *MAF2-5* on the bottom of chromosome 5) were found in up to 12 F_2 populations (Table 2). It is worth noting that our 6-week vernalization treatment did not eliminate the effects of *FRI* and *FLC*, the expression of which is strongly vernalization dependent (MICHAELS and AMASINO 1999; SHELDON *et al.* 1999). However, it has been shown before that accessions with an active *FLC* allele differ in their vernalization requirement, with much of this variation mapping to *FLC* itself (SHINDO *et al.* 2006).

QTL mapping to the *FLC* and *FRI* genomic regions were found in 11 and 8 of the 17 F_2 populations, respectively, and contribute about 19 and 12%, respectively, of the variance (Figure 3 and Table 2). The *MAF2–MAF5* cluster, which is very polymorphic between accessions and has been recently implicated in flowering-time variation (CAICEDO *et al.* 2009; ROSLOSKI *et al.* 2010), is a candidate for 8 QTL on the bottom of chromosome 5. These QTL can explain 15% of measured variance. Finally, the region containing the *FLC* ortholog *FLM*, which is deleted in the Nd-0 accession (WERNER *et al.* 2005), is included in 12 QTL explaining 15% of variance.

Overall, the 39 QTL associated with the genomic regions of *FRI* and the *FLC* clade contribute over 85% of explained variation. The remaining 15 QTL likely reflect accession-specific variation (Table 2). Two QTL studies have identified a QTL at *FT* (SHINDO *et al.* 2006; SCHWARTZ *et al.* 2009). One showed that Est-1 carries an allele that is less active than the reference allele (SCHWARTZ *et al.* 2009), and we could detect *FT* QTL in the Est-1 × RRS7 (P8) and Est-1 × Br-0 (P12) populations, which share Est-1 as one of the grandparents (Figures 3 and 6). Several modest QTL peaks were

TABLE 2

QTL cluster in our study

Population	*FLM*	*FRI*	*FLC*	*MAF2-MAF5*	Total variance (%)
Tamm-2 × Col-0 (P35)	Yes	Yes	Yes	Yes	35.3
Fei-0 × Col-0 (P66)	Yes			Yes	9.7
Sha × Fei-0 (P145)	Yes	Yes	Yes		31.2
Lov-5 × Sha (P2)			Yes		62.4
Bay-0 × Lov-5 (P19)		Yes	Yes		51.7
Bur-0 × Bay-0 (P3)	Yes	Yes	Yes	Yes	34.4
Bur-0 × Cvi-0 (P10)	Yes			Yes	39.7
Cvi-0 × RRS7 (P17)	Yes			Yes	37.9
Est-1 × RRS7 (P8)	Yes				25.2
Est-1 × Br-0 (P12)	Yes	Yes		Yes	50.9
Br-0 × C24 (P15)	Yes		Yes		39.6
C24 × RRS10 (P129)	Yes		Yes		61.6
Tsu-1 × RRS10 (P9)		Yes	Yes	Yes	64.3
Ts-1 × Tsu-1 (P169)	Yes			Yes	51.9
Van-0 × Bor-4 (P6)	Yes		Yes		20.75
NFA-8 ×x Van-0 (P7)		Yes	Yes		28.7
Bor-4 × NFA-8 (P20)		Yes	Yes		21.1
Total count	**12**	**8**	**11**	**8**	
Variance mean	**14.8%**	**12.1%**	**18.8%**	**13%**	**39.2**
Variance range	**3.4–35.7**	**5.9–18.5**	**4–53.5**	**3.2–32.5**	**9.7–64.3**

detected near *ERECTA*, and the *EARLY-FLOWERING 3* (*ELF3*) gene is a candidate causal locus (Hicks *et al.* 2001).

A broader comparison of our results from simple interval mapping with previously published QTL revealed that the *FRI*, *FLC*, *FLM*, and the *MAF2–MAF5* regions (Figure 6, Table 2, and Table 3) were probably shared with other studies (Alonso-Blanco *et al.* 1998; Werner *et al.* 2005; El-Lithy *et al.* 2006; O'neill *et al.* 2008). It is difficult to determine how well QTL detected in early studies overlap with our candidate genomic regions, as reported positions were not reported relative to the physical map (Alonso-Blanco *et al.* 1998; Loudet *et al.* 2002; Weinig *et al.* 2002; El-Lithy *et al.* 2004). More recent studies have, however, taken advantage of the Arabidopsis genome sequence information to generate a consensus physical map onto which QTL were mapped (El-Lithy *et al.* 2006; O'neill *et al.* 2008; Simon *et al.* 2008; Brachi *et al.* 2010). Many of the QTL identified with RILs over the past decade mapped to the same genomic regions and overlapped with the locations of *FLC* (13 instances), *FRI* (11), *MAF2-5* (11), and, to a lesser extent, with *FLM* (six times; Table 3). Mean explained variance in RILs contributed by *FRI* and the *FLC* clade reached 37.4%, very similar to the variance of 39.2% we observed to be associated with the same genomic regions (Tables 2 and 3). Additional QTL seen in RILs but not in our F_2 populations could explain another 20% of the standing variation, but these are likely to reflect single-gene variants specific for a parental accession. One example is the well-known loss-of-function allele at the receptor kinase gene *ERECTA* (*ER*) found in the accession Ler (a founding accession for 6 RILs; Table S5). We did not detect a significant QTL for *CRY2*, known to be functionally divergent in Cvi-0, the parent for two of our populations (Bur-0 × Cvi-0 [P10] and Cvi-0 × RRS7 [P17]), reflecting the short-day-dependent nature of the early flowering phenotype conferred by the $CRY2^{Cvi\text{-}0}$ allele (Figure 6C).

Evidence for allelic series within the *FLC* clade: The round-robin design (Figure S1) allowed us to draw a logic chain linking 14 of our founding accessions, and thus predict effects between accessions not directly connected in a cross. A clear gradient in the strength of *FLM*, *MAF2-5*, and *FLC* alleles was apparent (Figure 7), indicating that not only *FLC* (Shindo *et al.* 2006), but also other members of the *FLC* clade, contributed quantitatively to the observed variation in flowering time through allelic series.

The proposed allelic series generally agreed with the presence or absence of a QTL between two consecutive accessions. For example, large differences in effects separated the *FLM* locus of Col-0 and Fei-0 (grandparents of P66), as well as Fei-0 and Sha (grandparents of P145), but not those of Sha and Lov-5 (grandparents of P2). In agreement, a significant QTL was detected in the *FLM* region in P66 and P145, but not in P2 (Figure 3C). There were, however, some limitations of our analysis: the *FLM* QTL of Tsu-1 appeared to confer slightly later flowering than that of RRS10, but this difference in effect did not result in a QTL in the *FLM* region in the P9 population derived from these two parents (Figures 3 and 7A). The behavior of *MAF2* QTL also generally followed the predicted results from our QTL

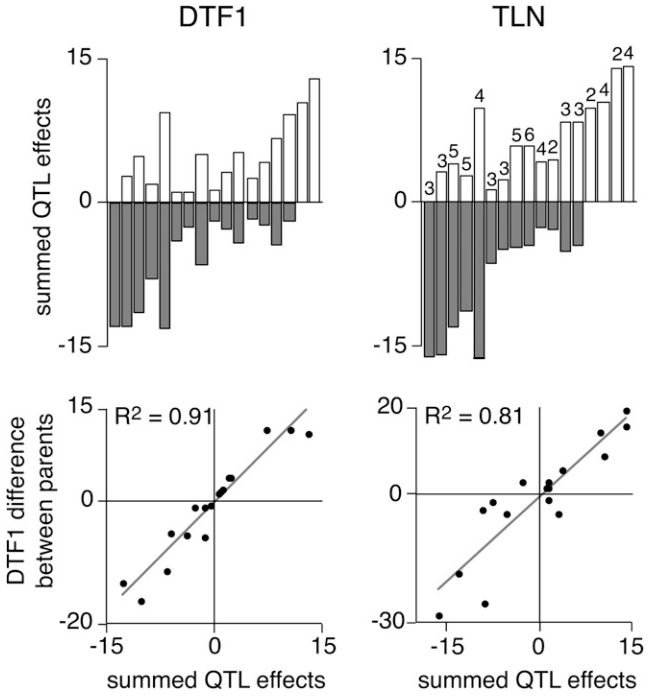

Figure 4.—Congruence between QTL effects and flowering-time difference of parents. Top, sum of negative (gray) and positive (white) effects; numbers indicate count of QTL. Bottom, correlation between summed QTL effects and difference in flowering time of parents.

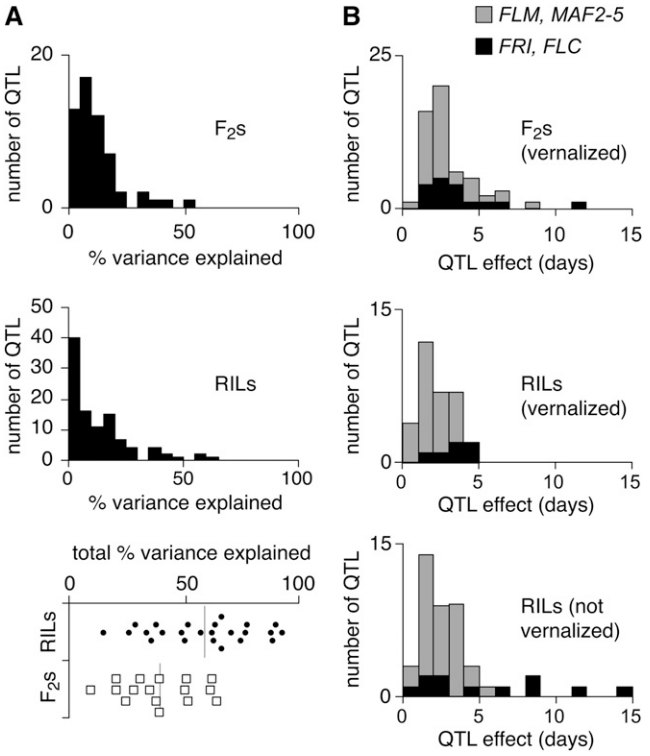

Figure 5.—Comparison of the power for QTL discovery in F_2 populations and RILs. (A) Variance explained by individual or all QTL in our F_2 populations and in RILs (see Figure 6). Because of our significance threshold for QTL, individual QTL explain at least 3% of the total variance, while RIL QTL may explain less. Gray line indicates mean for all populations. (B) Relative contribution of QTL at either *FRI* and *FLC* or *FLM* and *MAF2-5*.

discovery (Figure 7B), although a very-late-flowering *FLC* QTL, on the top of chromosome 5, appeared to mask *MAF2* QTL effects on the bottom of chromosome 5. Populations lacking a QTL near *MAF2* but showing strong differences in effect for the parental alleles of this region share the Lov-5 accession, which has a very-late-flowering *FLC* QTL. Only following composite interval mapping was a QTL detected in the *MAF2* region, and only in the Bay-0 × Lov-5 population (P19). This does not reflect a missed epistatic interaction, as we could not detect any epistasis between the upper and lower arm of chromosome 5 in Lov-5 × Sha (P2) or P19. It is worth noting that $FLC^{\text{Lov-5}}$ confers the strongest effects among our populations, especially in the P2 population with a measured effect of 11.5 days for the trait DTF1.

The allelic series of the QTL at *FLC* was dominated by the very strong effects associated with $FLC^{\text{Lov-5}}$ and FLC^{RRS10} (Figure 7C). FLC^{C24} is probably not inactive, as was previously indicated by crosses to plants with known functional or inactive alleles of *FLC* (Sanda and Amasino 1996). When C24 is crossed to *flc-3*, an *FLC* loss-of-function allele in Col-0, a fraction of F_2 plants exhibited a late-flowering phenotype that cosegregates with FLC^{C24} (not shown). In addition, a flowering-time QTL was detected around the *FRI* region in a Col-0 × C24 RIL set, while no QTL was found around the *FLC* region in the same population, indicating that the Col-0 and C24 alleles of *FLC* are similar (S. Balasubramanian, T. Altmann and D. Weigel, unpublished results). C24 might therefore carry a functional *FLC* copy whose effect is canceled by an extragenic modifier.

The observed gradient in flowering time caused by the parental alleles at the *FLM*, *MAF2*, and *FLC* loci suggested that the late-flowering accessions might not share the same allele but instead each carry a rare allele. We attempted to test this hypothesis by querying existing sequence data sets. Clark and Colleagues (2007) determined polymorphisms in all founding accessions. The oligonucleotide-based resequencing technology, however, revealed only about half of all coding SNPs and a considerably smaller portion of noncoding SNPs. It was therefore not surprising that the presence of a Clark SNP between two accessions (regardless of their position: promoter, coding sequence, or within introns) was not correlated with the existence of a QTL for any of our candidates (Table S6, Table S7, Table S8). Available sequence information at the *MAF2–MAF5* gene cluster is unfortunately of limited use in our case, as only two of our accessions are represented in the 168 accessions characterized by Caicedo and Colleagues (2009). The current resolution in known common polymorphisms therefore suggests an allelic series contributed by rare alleles for our candidate genes rather than

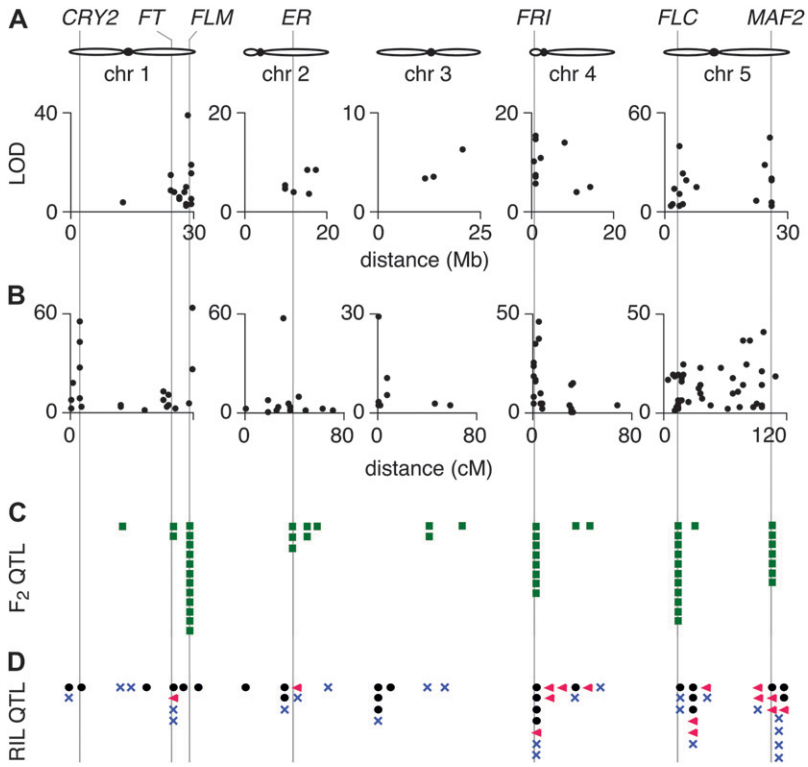

FIGURE 6.—Comparison of flowering-time QTL mapping in F_2 populations (this study) and published RIL populations. (A) Fifty-five QTL from simple interval mapping of F_2 populations (this study). (B) QTL from the analysis of published RIL populations. (C) QTL locations in F_2 populations (this study, green squares). (D) QTL locations in RIL studies: solid circles (LOUDET *et al.* 2002; EL-LITHY *et al.* 2004, 2006; WERNER *et al.* 2005); pink triangles (O'NEILL *et al.* 2008); blue X's (SIMON *et al.* 2008). In all cases, detected QTL are for days to flower (DTF1).

a single SNP segregating in our F_2 populations with a QTL at a given flowering-time candidate locus.

DISCUSSION

The control of flowering time in *A. thaliana* has been the focus of much study over the past decade. Yet, despite the wealth of resources at our disposal, a clear picture of the species-wide genetic architecture of flowering time has not yet emerged, since the simultaneous analysis of populations representing several parents has been the exception (SIMON *et al.* 2008; KOVER *et al.* 2009; BRACHI *et al.* 2010).

Most of the previous work mapping flowering-time QTL has used RILs. Because RILs represent immortalized, largely fixed recombinant genotypes that can be

TABLE 3

QTL candidates in other studies

Reference	*FLM*	*FRI*	*FLC/CO*	*MAF2–MAF5*	Total variance (%)
ALONSO-BLANCO *et al.* (1998)			Yes	Yes	28.3
WEINIG *et al.* (2002)			Yes	Yes	34
LOUDET *et al.* (2002)		Yes	Yes		52
EL-LITHY *et al.* (2004)	Yes	Yes	Yes	Yes	53.5
WERNER *et al.* (2005)	Yes				26.6
EL-LITHY *et al.* (2006)		Yes	Yes		29.6
EL-LITHY *et al.* (2006)	Yes	Yes	Yes	Yes	52.5
EL-LITHY *et al.* (2006)		Yes	Yes	Yes	52.2
SIMON *et al.* (2008)		Yes		Yes	21
SIMON *et al.* (2008)	Yes	Yes	Yes	Yes	18
SIMON *et al.* (2008)	Yes			Yes	28
SIMON *et al.* (2008)			Yes	Yes	12
SIMON *et al.* (2008)			Yes	Yes	32
O'NEILL *et al.* (2008)	Yes	Yes	Yes		55.3
O'NEILL *et al.* (2008)		Yes	Yes		29
O'NEILL *et al.* (2008)		Yes			38
O'NEILL *et al.* (2008)		Yes	Yes	(Yes)	64
O'NEILL *et al.* (2008)				Yes	37
O'NEILL *et al.* (2008)	—	—	—	—	
Total count	**6**	**11**	**13**	**11 (12)**	
Variance mean	**11.5%**	**21.5%**	**12.7%**	**14.2 (15.2)%**	**37.4**
Variance range	**3–26.6**	**5–46.6**	**2–48**	**2–37**	**12–64**

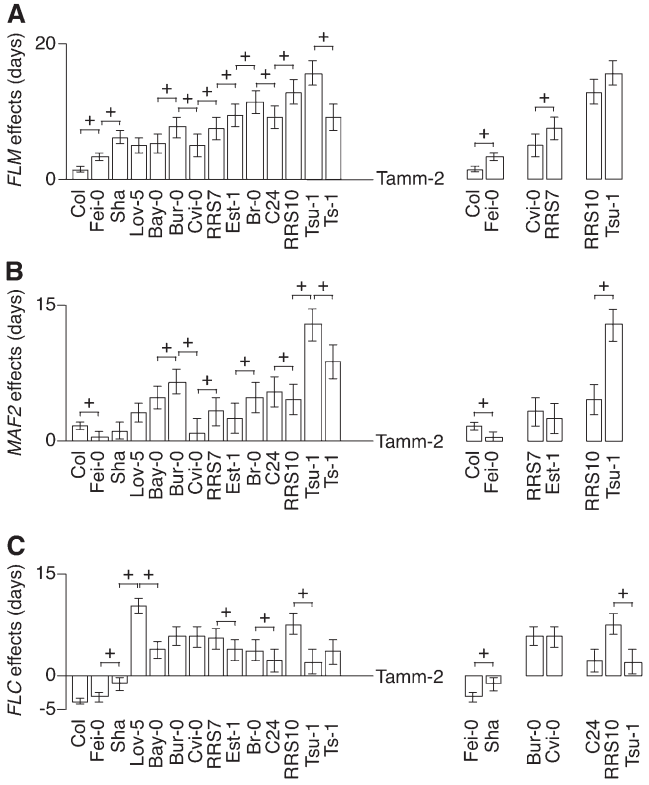

FIGURE 7.—Allelic series among QTL at members of the *FLC* clade. Effects relative to the Tamm-2 allele were plotted along the logic chain of our simple round-robin crossing design, and then added up. + indicates detected QTL. (A) *FLM* effects, (B) *MAF2* effects, and (C) *FLC* effects.

phenotyped many times, genotyping costs could be amortized over many phenotyping trials. In the past few years, expenses associated with genotyping have dropped considerably, and adoption of next-generation sequencing platforms promises to further lower costs while increasing the resolution of genotyping (*e.g.*, BAIRD *et al.* 2008; HUANG *et al.* 2009; XIE *et al.* 2010). Apart from marker analysis, polymorphism discovery used to be a major bottleneck, before the advent of ultra-high-resolution microarrays and new sequencing methods (CLARK *et al.* 2007; OSSOWSKI *et al.* 2008). We have investigated the potential of F_2 populations as an alternative to immortal RILs, by making full use of our knowledge of hundreds of thousands of polymorphisms described for 20 accessions (CLARK *et al.* 2007).

The major QTL that we detected could explain on average about 40% of the overall variation, indicating that the remaining 60% of flowering-time variation must be associated with modest-effect QTL that lie below our significance threshold. That the unexplained variance does not hinder us from predicting the parental flowering times suggests that the remaining effects must be (1) very small, and therefore remain undetectable in our populations, and (2) equally distributed between negative and positive effects, thus canceling each other out. We also observed extensive variation in the onset of flowering in all F_2 populations, even when the parental accessions flowered at very similar times. Because hybridization of *A. thaliana* accessions occurs regularly in the wild (ABBOTT and GOMES 1989; BERGELSON *et al.* 1998; NORDBORG *et al.* 2005; PICÓ *et al.* 2008), our results have important implications for the initial stages of adaptation via flowering time.

We also compared our results to a recently published species-wide study of flowering-time QTL in maize. In our populations, 54 of 55 QTL alleles altered flowering time by at least 1 day, while this was true for only 7 of 333 QTL in maize (Figure S4, BUCKLER *et al.* 2009). In *A. thaliana*, an average of 3–4 QTL per F_2 population explained 3.1–22.7 days difference in flowering (mean 10.1 days), while the combined effects of 13–14 maize QTL per population in maize ranged from 1.5 to 13.0 (mean 6.2).

Also in contrast to maize, a small number of regions was overrepresented for flowering-time QTL. Two of them include *FRI* and *FLC*, although our F_2 populations were all exposed to prolonged cold in an attempt to identify vernalization-independent loci. Variation at the *FRI* region strongly contributed to flowering-time variation in RILs, reaching values as high as 46%, and averaging 21.5% across all RILs. The relative importance of the *FRI* genomic region in our 17 F_2 populations was not quite as strong, averaging only 12.1% of total variance, and was never higher than 19%, indicating that 6 weeks of vernalization was effective in limiting the contribution of FRI to flowering time. QTL mapping to the *FLC* genomic region explained between 4 and 53.5% of the standing variation in our populations (Table 2), and between 2 and 37% in RILs (Table 3), confirming *FLC* as a major gene for flowering time. Lov-5 carries a strong, vernalization-insensitive *FLC* allele (SHINDO *et al.* 2006), which may skew the mean and range associated with *FLC*: after removal of $FLC^{Lov\text{-}5}$ from our list, mean variance dropped to 13.3 (range of 4–41.5) and was then more in line with results obtained with RILs. Two additional regions where QTL clustered overlapped with the locations of the remaining members of the *FLC* clade, *FLM,* and *MAF2-5*, in both our F_2 and RIL populations. Mean variance and range were comparable in both sets of populations, suggesting that the observed allelic series at *FLM* and *MAF2-5* between 14 of our 18 founding accessions might also apply to the RIL parental accessions as well. We detected QTL overlapping with the *FLM* genomic regions twice as often as in RIL studies, possibly reflecting the partial bias in RIL parental accessions. Indeed, the common laboratory accessions Col and Ler were crossed, either to each other or to other accessions, to create 12 of the 19 RIL populations characterized for flowering-time QTL (Table S5). In field experiments such as BRACHI and COLLEAGUES (2010),

the decision to flower results from the integration of daily temperature cycles and gradual photoperiod changes. Only under these conditions—where daily temperatures often did not raise above 10°—were QTL in genes associated with the circadian clock detected, indicating that low temperatures may define a sensitized condition for variation in clock function in the specific context of flowering time. In all other studies, including this study, growth conditions included a constant temperature >16° and long and nonchanging photoperiods sufficient to saturate the photoperiodic pathway, thus allowing the emergence of effects caused by general mediators of flowering time and providing an explanation for the absence of clock-associated loci in our list of QTL.

Although we vernalized seedlings for 6 weeks before release at 16°, we still detected QTL mapping to the *FRI*, *FLC*, and *FLM/MAF2-5* genomic regions. Our growth chambers maintain very good control of temperature, light intensity, and air humidity, which likely greatly limited phenotypic variation due to microenvironmental noise and therefore enhanced our ability to detect QTL. In addition, the relatively low temperature of 16° generally delays flowering in long days compared to 23° (Lempe *et al.* 2005). Responses to ambient temperature involve *SVP*, as demonstrated by a similar flowering time at 16° and 23° for *svp* mutants (Lee *et al.* 2007). SVP function is dependent on FLM, as an *svp* loss of function can suppress the late flowering caused by *FLM* overexpression (Scortecci *et al.* 2003). It is thus conceivable that *flm* mutants might be similarly insensitive to changes in ambient temperature and that growing plants at 16° allowed us to measure differences in the strength of *FLM* alleles that had escaped detection in several previous studies.

Although two of our major QTL clusters overlap with the locations of *FLM* and *MAF2-5*, initial genome-wide association studies failed to identify significant SNPs at either *FLM* or *MAF2–MAF5* (Atwell *et al.* 2010; Brachi *et al.* 2010). Genome-wide association studies fail when they include too few accessions with functionally variant alleles, or if too many of the functionally variant alleles are distinct from each other. The evidence for allelic series at all our QTL is in support of the latter hypothesis. Only after an increase in sample size from 96 to 473 unique accessions did *MAF2* emerge as a possible flowering-time QTL candidate following association mapping (Li *et al.* 2010). In all cases described in Arabidopsis, one constant feature remains: QTL for flowering time are few, but are associated with large effects.

The chromosomal location of most strong-effect QTL is in itself quite striking: aside from *ER*, which is close to the centromere of chromosome 2, all other flowering-time QTL candidate genes (*FLC*, *FLM*, *MAF2-5*, and *FRI*) are located at the ends of their respective chromosomes. Following hybridization, parental genomes recombine and segregate to form novel combinations of alleles in the progeny. The low frequency of crossovers each generation means that large, intact fragments of parental chromosome will be transmitted to the progeny. The large-effect QTL that we detected in our populations would thus generate distinct pools of alleles in the F_2 and subsequent generations, which could have adaptive significance due to variation in flowering time. On the other hand, growth-related traits tend to display more complex genetic architectures than flowering time, with many small-effect QTL, and are often ripe with epistatic interactions (Vlad *et al.* 2010). This delicate balance of alleles will be severely disrupted after hybridization and formation of pools of early and late-flowering plants; however, positioning flowering-time QTL to ends of chromosomes will limit the extent of genetic drag imposed on the rest of the chromosome.

In conclusion, we have identified a small number of genomic regions with strong effects on flowering time. Some of the same regions, and indeed candidate genes, are now coming to the forefront through genome-wide association mapping studies. That *FLM* has yet to be described as being associated with flowering-time variation in association studies might mean only that the number of accessions remains too small, if many rare alleles contribute. The complete sequencing of hundreds, and soon thousands, of genomes from *A. thaliana* accessions (Weigel and Mott 2009) is a prerequisite for the genome-wide annotation of potential functional polymorphisms; apart from the direct analysis of QTL candidates, this will also improve the power of genome-wide association studies, since alleles that are the consequence of convergent changes in activity can be combined.

We thank Richard Clark and Suresh Balasubramanian for discussions during the design stages of the project. We also are indebted to Josip Perkovič, Hannah Helms, Waldemar Hauf, and Marcella Amorim for help with phenotyping and seed collection. K.B. and D.W. conceived and designed the experiments, P.A.S., K.B., R.A.E.L., and L.Y. performed the experiments, P.A.S. and R.M. analyzed the data, and P.A.S. and D.W. wrote the paper. This research was supported by postdoctoral fellowships from the European Molecular Biology Organization (P.A.S.), National Institutes of Health (K.B.), Human Frontiers Science Program (R.A.E.L.), grant FP6 IP AGRONOMICS (contract LSHG-CT-2006-037704), from a Gottfried Wilhelm Leibniz Award of the Deutsche Forschungsgemeinschaft, and the Max Planck Society (D.W.).

LITERATURE CITED

Abbott, R. J., and M. F. Gomes, 1989 Population genetic structure and outcrossing rate of *Arabidopsis thaliana* (L.) Heynh. Heredity **62:** 411–418.

Alonso-Blanco, C., S. E. El-Assal, G. Coupland and M. Koornneef, 1998 Analysis of natural allelic variation at flowering time loci in the Landsberg erecta and Cape Verde Islands ecotypes of Arabidopsis thaliana. Genetics **149:** 749–764.

Amasino, R., 2010 Seasonal and developmental timing of flowering. Plant J. **61:** 1001–1013.

Atwell, S., Y. S. Huang, B. J. Vilhjalmsson, G. Willems, M. Horton *et al.*, 2010 Genome-wide association study of 107 phenotypes in *Arabidopsis thaliana* inbred lines. Nature **465:** 627–631.

Baird, N. A., P. D. Etter, T. S. Atwood, M. C. Currey, A. L. Shiver *et al.*, 2008 Rapid SNP discovery and genetic mapping using sequenced RAD markers. PLoS One **3:** e3376.

Balasubramanian, S., S. Sureshkumar, M. Agrawal, T. P. Michael, C. Wessinger *et al.*, 2006 The PHYTOCHROME C photoreceptor gene mediates natural variation in flowering and growth responses of Arabidopsis thaliana. Nat. Genet. **38:** 711–715.

Bäurle, I., and C. Dean, 2006 The timing of developmental transitions in plants. Cell **125:** 655–664.

Bergelson, J., E. Stahl, S. Dudek and M. Kreitman, 1998 Genetic variation within and among populations of *Arabidopsis thaliana*. Genetics **148:** 1311–1323.

Brachi, B., N. Faure, M. Horton, E. Flahauw, A. Vazquez *et al.*, 2010 Linkage and association mapping of *Arabidopsis thaliana* flowering time in nature. PLoS Genet. **6:** e1000940.

Broman, K. W., H. Wu, S. Sen and G. A. Churchill, 2003 R/qtl: QTL mapping in experimental crosses. Bioinformatics **19:** 889–890.

Buckler, E. S., J. B. Holland, P. J. Bradbury, C. B. Acharya, P. J. Brown *et al.*, 2009 The genetic architecture of maize flowering time. Science **325:** 714–718.

Caicedo, A. L., C. Richards, I. M. Ehrenreich and M. D. Purugganan, 2009 Complex rearrangements lead to novel chimeric gene fusion polymorphisms at the *Arabidopsis thaliana MAF2–5* flowering time gene cluster. Mol. Biol. Evol. **26:** 699–711.

Clark, R. M., G. Schweikert, C. Toomajian, S. Ossowski, G. Zeller *et al.*, 2007 Common sequence polymorphisms shaping genetic diversity in *Arabidopsis thaliana*. Science **317:** 338–342.

El-Din El-Assal, S., C. Alonso-Blanco, A. J. Peeters, V. Raz and M. Koornneef, 2001 A QTL for flowering time in Arabidopsis reveals a novel allele of CRY2. Nat. Genet. **29:** 435–440.

El-Lithy, M. E., E. J. Clerkx, G. J. Ruys, M. Koornneef and D. Vreugdenhil, 2004 Quantitative trait locus analysis of growth-related traits in a new *Arabidopsis* recombinant inbred population. Plant Physiol. **135:** 444–458.

El-Lithy, M. E., L. Bentsink, C. J. Hanhart, G. J. Ruys, D. Rovito *et al.*, 2006 New Arabidopsis recombinant inbred line populations genotyped using SNPWave and their use for mapping flowering-time quantitative trait loci. Genetics **172:** 1867–1876.

Filiault, D. L., C. A. Wessinger, J. R. Dinneny, J. Lutes, J. O. Borevitz *et al.*, 2008 Amino acid polymorphisms in *Arabidopsis* phytochrome B cause differential responses to light. Proc. Natl. Acad. Sci. USA **105:** 3157–3162.

Greenup, A., W. J. Peacock, E. S. Dennis and B. Trevaskis, 2009 The molecular biology of seasonal flowering-responses in *Arabidopsis* and the cereals. Ann. Bot. **103:** 1165–1172.

Hicks, K. A., T. M. Albertson and D. R. Wagner, 2001 EARLY FLOWERING3 encodes a novel protein that regulates circadian clock function and flowering in Arabidopsis. Plant Cell **13:** 1281–1292.

Huang, X., Q. Feng, Q. Qian, Q. Zhao, L. Wang *et al.*, 2009 High-throughput genotyping by whole-genome resequencing. Genome Res. **19:** 1068–1076.

Johanson, U., J. West, C. Lister, S. Michaels, R. Amasino *et al.*, 2000 Molecular analysis of *FRIGIDA*, a major determinant of natural variation in *Arabidopsis* flowering time. Science **290:** 344–347.

Jurinke, C., D. van den Boom, C. R. Cantor and H. Koster, 2001 Automated genotyping using the DNA MassArray technology. Methods Mol. Biol. **170:** 103–116.

Kobayashi, Y., and D. Weigel, 2007 Move on up, it's time for change: mobile signals controlling photoperiod-dependent flowering. Genes Dev. **21:** 2371–2384.

Kover, P. X., W. Valdar, J. Trakalo, N. Scarcelli, I. M. Ehrenreich *et al.*, 2009 A multiparent advanced generation inter-cross to fine-map quantitative traits in *Arabidopsis thaliana*. PLoS Genet. **5:** e1000551.

Lee, J. H., S. J. Yoo, S. H. Park, I. Hwang, J. S. Lee *et al.*, 2007 Role of SVP in the control of flowering time by ambient temperature in Arabidopsis. Genes Dev. **21:** 397–402.

Lempe, J., S. Balasubramanian, S. Sureshkumar, A. Singh, M. Schmid *et al.*, 2005 Diversity of flowering responses in wild *Arabidopsis thaliana* strains. PLoS Genet. **1:** e6–0109–0118.

Li, Y., Y. Huang, J. Bergelson, M. Nordborg and J. O. Borevitz, 2010 Association mapping of local climate-sensitive quantitative trait loci in Arabidopsis thaliana. Proc. Natl. Acad. Sci. USA **107:** 21199–21204.

Loudet, O., S. Chaillou, C. Camilleri, D. Bouchez and F. Daniel-Vedele, 2002 Bay-0 × Shahdara recombinant inbred line population: a powerful tool for the genetic dissection of complex traits in *Arabidopsis*. Theor. Appl. Genet. **104:** 1173–1184.

Michaels, S. D., and R. M. Amasino, 1999 *FLOWERING LOCUS C* encodes a novel MADS domain protein that acts as a repressor of flowering. Plant Cell **11:** 949–956.

Nordborg, M., T. T. Hu, Y. Ishino, J. Jhaveri, C. Toomajian *et al.*, 2005 The pattern of polymorphism in *Arabidopsis thaliana*. PLoS Biol. **3:** e196.

O'Neill, C. M., C. Morgan, J. Kirby, H. Tschoep, P. X. Deng *et al.*, 2008 Six new recombinant inbred populations for the study of quantitative traits in *Arabidopsis* thaliana. Theor. Appl. Genet. **116:** 623–634.

Ossowski, S., K. Schneeberger, R. M. Clark, C. Lanz, N. Warthmann *et al.*, 2008 Sequencing of natural strains of *Arabidopsis thaliana* with short reads. Genome Res. **18:** 2024–2033.

Picó, F. X., B. Mendez-Vigo, J. M. Martinez-Zapater and C. Alonso-Blanco, 2008 Natural genetic variation of *Arabidopsis thaliana* is geographically structured in the Iberian peninsula. Genetics **180:** 1009–1021.

Ratcliffe, O. J., G. C. Nadzan, T. L. Reuber and J. L. Riechmann, 2001 Regulation of flowering in *Arabidopsis* by an *FLC* homologue. Plant Physiol. **126:** 122–132.

Ratcliffe, O. J., R. W. Kumimoto, B. J. Wong and J. L. Riechmann, 2003 Analysis of the Arabidopsis MADS AFFECTING FLOWERING gene family: MAF2 prevents vernalization by short periods of cold. Plant Cell **15:** 1159–1169.

Rosloski, S. M., S. S. Jali, S. Balasubramanian, D. Weigel and V. Grbic, 2010 Natural diversity in flowering responses of *Arabidopsis thaliana* caused by variation in a tandem gene array. Genetics **186:** 263–276.

Sanda, S. L., and R. Amasino, 1996 Genetic and physiological analysis of flowering time in the C24 line of *Arabidopsis thaliana*. Weeds World **2:** 2–8.

Schwartz, C., S. Balasubramanian, N. Warthmann, T. P. Michael, J. Lempe *et al.*, 2009 Cis-regulatory changes at *FLOWERING LOCUS T* mediate natural variation in flowering responses of *Arabidopsis thaliana*. Genetics **183:** 723–732.

Scortecci, K., S. D. Michaels and R. M. Amasino, 2003 Genetic interactions between *FLM* and other flowering-time genes in *Arabidopsis thaliana*. Plant Mol. Biol. **52:** 915–922.

Sheldon, C. C., J. E. Burn, P. P. Perez, J. Metzger, J. A. Edwards *et al.*, 1999 The *FLF* MADS box gene: a repressor of flowering in Arabidopsis regulated by vernalization and methylation. Plant Cell **11:** 445–458.

Shindo, C., M. J. Aranzana, C. Lister, C. Baxter, C. Nicholls *et al.*, 2005 Role of *FRIGIDA* and *FLOWERING LOCUS C* in determining variation in flowering time of *Arabidopsis*. Plant Physiol. **138:** 1163–1173.

Shindo, C., C. Lister, P. Crevillen, M. Nordborg and C. Dean, 2006 Variation in the epigenetic silencing of *FLC* contributes to natural variation in *Arabidopsis* vernalization response. Genes Dev. **20:** 3079–3083.

Simon, M., O. Loudet, S. Durand, A. Berard, D. Brunel *et al.*, 2008 Quantitative trait loci mapping in five new large recombinant inbred line populations of *Arabidopsis thaliana* genotyped with consensus single-nucleotide polymorphism markers. Genetics **178:** 2253–2264.

Turck, F., F. Fornara and G. Coupland, 2008 Regulation and identity of florigen: FLOWERING LOCUS T moves center stage. Annu. Rev. Plant Biol. **59:** 573–594.

Vlad, D., F. Rappaport, M. Simon and O. Loudet, 2010 Gene transposition causing natural variation for growth in *Arabidopsis thaliana*. PLoS Genet. **6:** e1000945.

Wang, Q., U. Sajja, S. Rosloski, T. Humphrey, M. C. Kim *et al.*, 2007 *HUA2* caused natural variation in shoot morphology of *A. thaliana*. Curr. Biol. **17:** 1513–1519.

Weigel, D., and R. Mott, 2009 The 1001 Genomes Project for *Arabidopsis thaliana*. Genome Biol. **10:** 107.

Weinig, C., M. C. Ungerer, L. A. Dorn, N. C. Kane, Y. Toyonaga *et al.*, 2002 Novel loci control variation in reproductive timing in *Arabidopsis thaliana* in natural environments. Genetics **162:** 1875–1884.

Werner, J. D., J. O. Borevitz, N. Warthmann, G. T. Trainer, J. R. Ecker *et al.*, 2005 Quantitative trait locus mapping and DNA array hybridization identify an *FLM* deletion as a cause for natural flowering-time variation. Proc. Natl. Acad. Sci. USA **102:** 2460–2465.

Xie, W., Q. Feng, H. Yu, X. Huang, Q. Zhao *et al.*, 2010 Parent-independent genotyping for constructing an ultrahigh-density linkage map based on population sequencing. Proc. Natl. Acad. Sci. USA **107:** 10578–10583.

Yandell, B. S., T. Mehta, S. Banerjee, D. Shriner, R. Venkataraman *et al.*, 2007 R/qtlbim: QTL with Bayesian Interval Mapping in experimental crosses. Bioinformatics **23:** 641–643.

Communicating editor: M. Kirst

GENETICS

Supporting Information
http://www.genetics.org/cgi/content/full/genetics.111.126607/DC1

Genetic Architecture of Flowering-Time Variation in *Arabidopsis thaliana*

Patrice A. Salomé, Kirsten Bomblies, Roosa A. E. Laitinen, Levi Yant, Richard Mott and Detlef Weigel

DOI: 10.1534/genetics.111.126607

FILE S1

Supporting Methods

Calibration of variance: Before carrying out an exhaustive search of QTL associated with flowering time, we wished to determine how well our F_2 populations would behave. To this end, we chose two clear phenotypes with strong candidates genes: the glabrous phenotype of the Br-0 accession, and the *erecta*-like phenotype of the Van-0 accession. We scored the absence of trichomes on leaves of F_2 plants from the P12 population, in which Br-0 was crossed to Est-1, an accession with normal trichome density. The segregation ratio between glabrous and "hairy" plants fit perfectly that expected for a simple Mendelian recessive trait (122 glabrous and 339 hairy, $\chi^2 = 0.5$). Performing a genome-wide association of the glabrous phenotype against the P12 genotypes identified a single chromosomal region on chromosome 3 with an LOD score of 100.6 that could explain 99.4% of the total variation (Figure S3A). The SNP showing the strongest linkage with the glabrous phenotype in the Br-0 background was located 4,594 bp downstream of the *GLABRA1* (*GL1*) gene, an obvious candidate for the causal gene inactivated in Br-0.
We confirmed the power of our populations with the *erecta*-like phenotype displayed by Van-0. Again, we scored F_2 plants for *erecta*-like leaf shape and inflorescences in the P6 (Van-0 x Bor-4) and P7 (NFA-8 x Van-0) populations. Only a single genomic region showed strong association with this phenotype, with LOD scores of 68 for P6 and 62 for P7. This region mapped to the *ERECTA* (*ER*) gene, whose loss-of-function allele in the Landsberg *erecta* (Ler) accession was the namesake of the selected phenotype; a cross Ler and Van-0 failed to rescue the *erecta*-like phenotypes of Van-0, demonstrating that the two loci are likely allelic (Figure S3B and C). In both populations, the amount of variance explained by this single causal locus could account for 79% (for P6) and 72 % for P7

File S2

Genotypes and phenotypes of the 17 Arabidopsis F_2 populations described in this study

File S2 is available for download as a compressed folder (.zip) at http://www.genetics.org/cgi/content/full/genetics.111.126607/DC1.

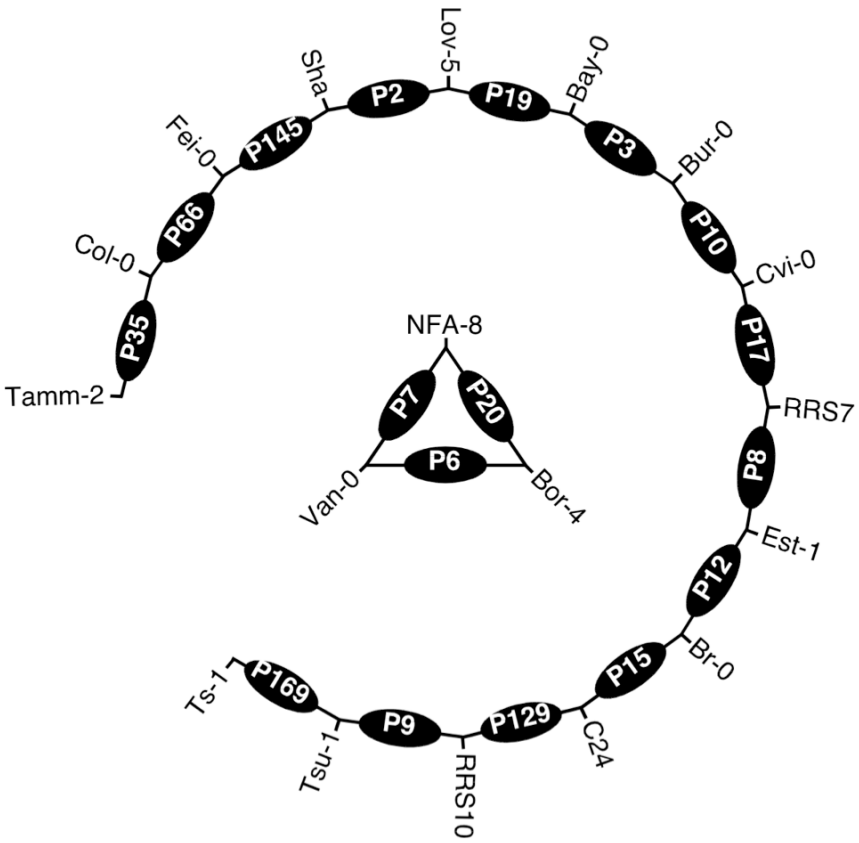

FIGURE S1.–Crossing design. The 17 grandparents are shown, with the resulting population name indicated in the black ovals. Note that the position of the accession relative to the ovals does not indicate directionality of the cross.

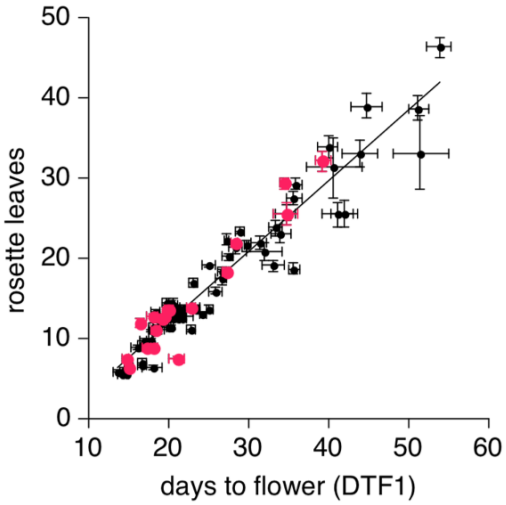

FIGURE S2.–Correlation between days to flower and rosette leaf number in the 96 NORDBORG accessions (NORDBORG *et al.* 2005). Mean values and 95% confidence intervals are shown.

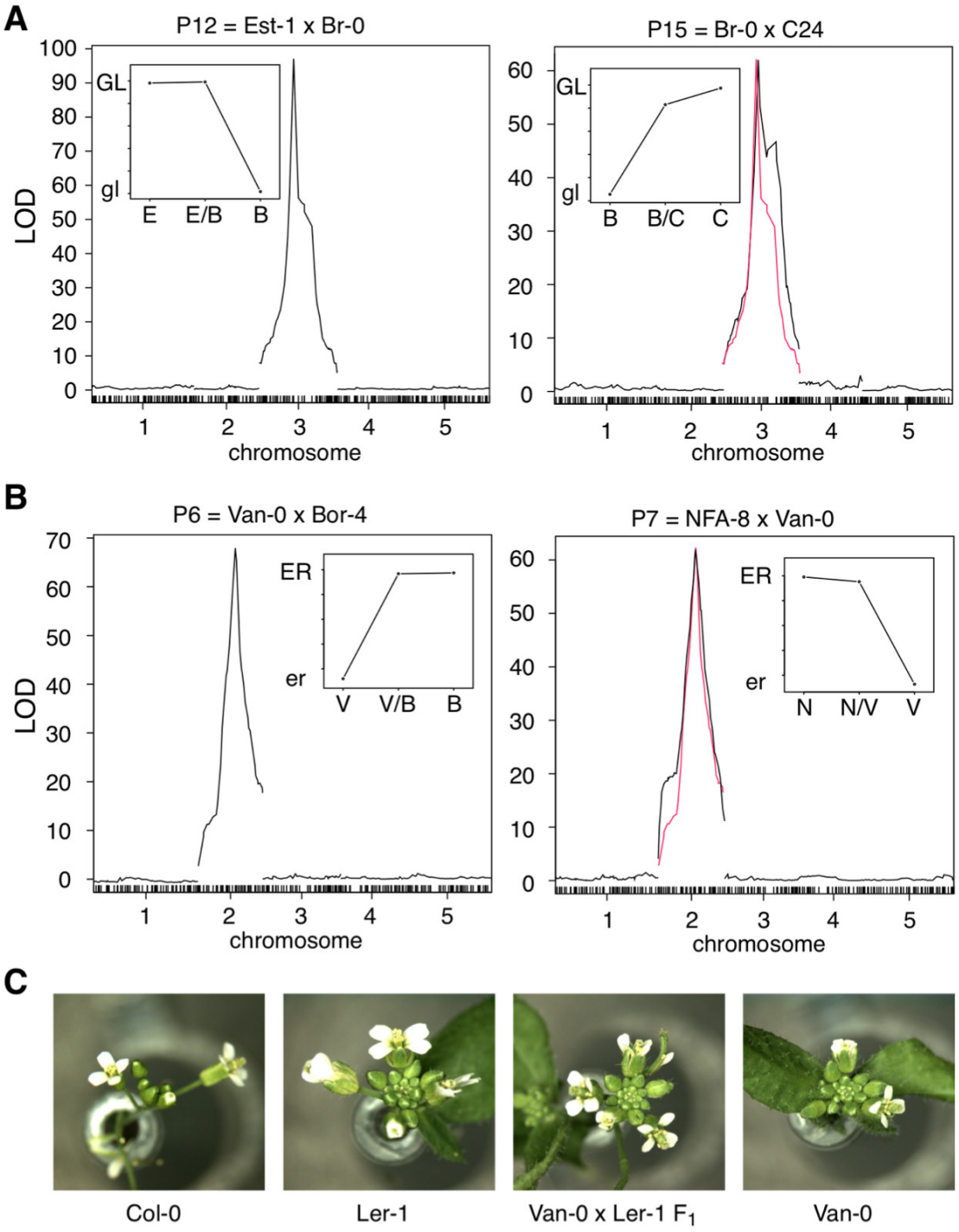

FIGURE S3.–Calibrating the detection of QTL with single-gene recessive traits. (A) QTL maps for the glabrous phenotype observed in Br-0 in the F_2 populations P12 and P15. In both cases, a single QTL is detected at the *GL1* locus on chromosome 3. Insets: effect plots associated with the two alleles at the *GL1* locus. (B) QTL maps for the erecta-like leaf shape and inflorescence phenotype seen in Van-0 in the F_2 populations P6 and P7. In both cases, a single QTL peak is obtained, mapping to the *ER* locus. Inset: effect plots associated with the two alleles at the *ER* locus. (C) Confirmation that Van-0 carries a non-functional copy of *ERECTA* by non-complementation. Shown here are representative pictures of single plants from Col-0, Ler-1, Van-0 x Ler-1 F_1 and Van-0. The inflorescences of the same genotypes were photographed later, and show that the inflorescence phenotypes or Ler-1 and Van-0 are allelic.

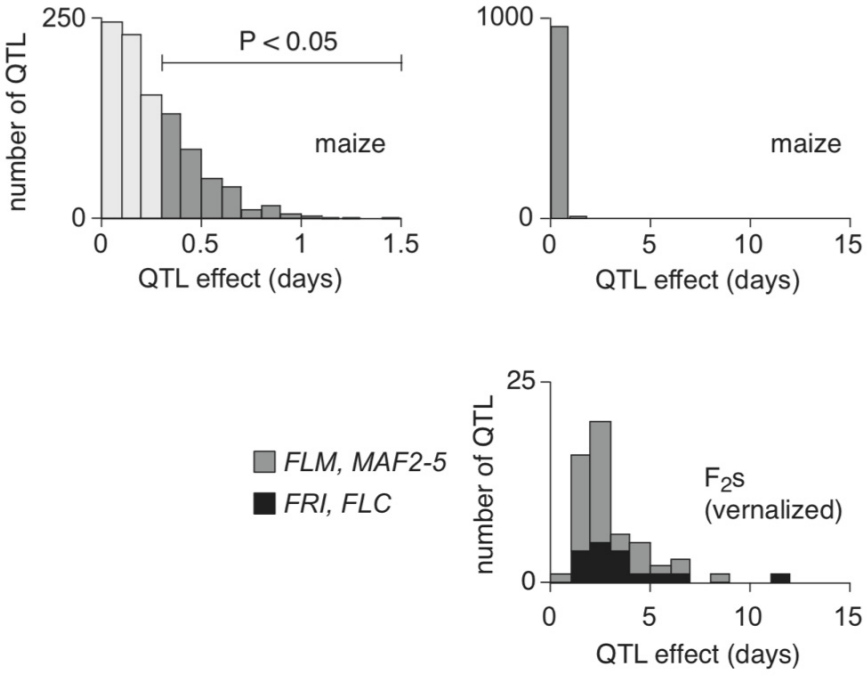

FIGURE S4.–Comparison of absolute QTL effects between our study and maize (BUCKLER *et al.* 2009). In all cases, detected QTL are for days to flower (DTF1).

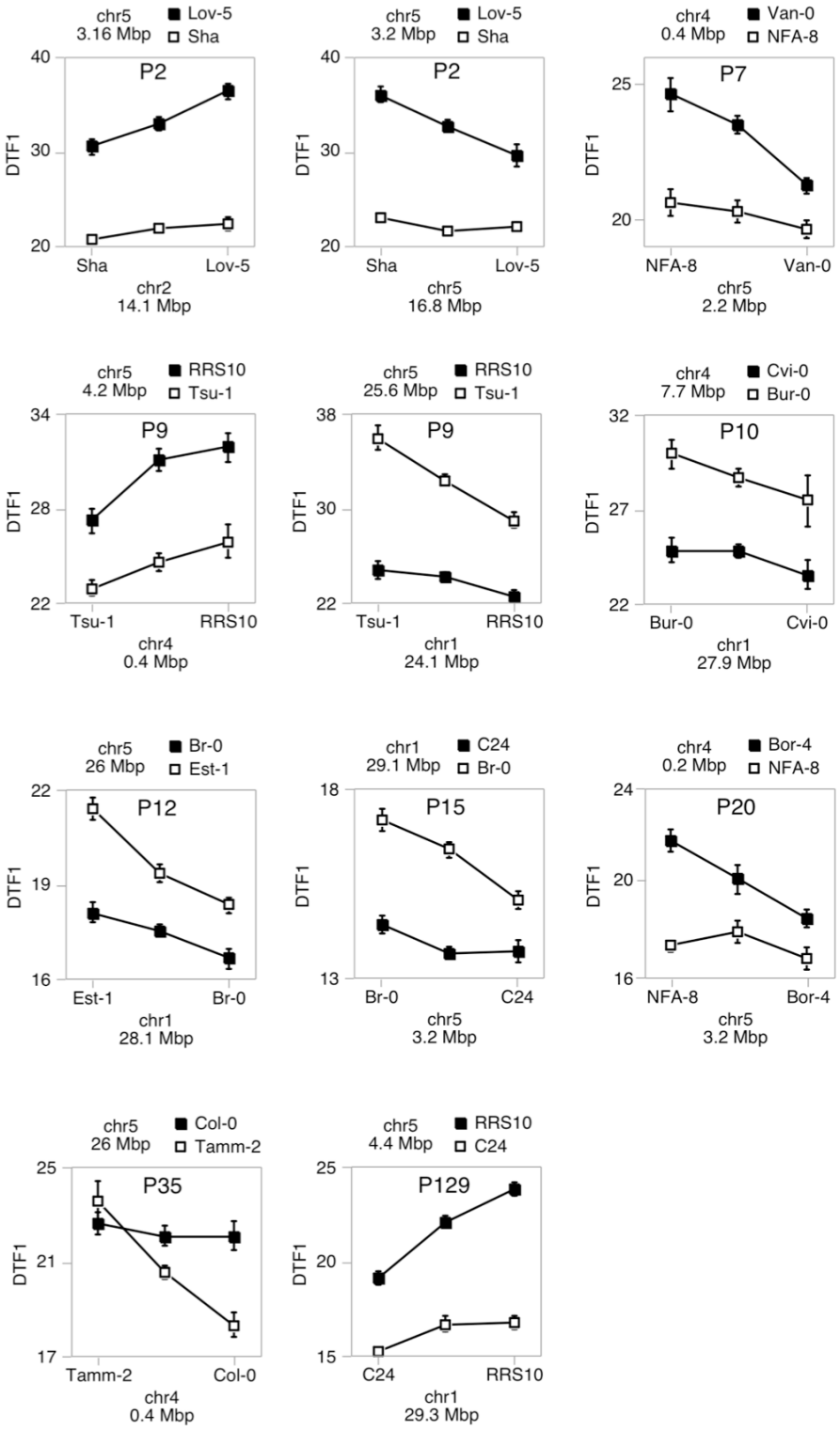

FIGURE S5.–Epistatic interactions detected between flowering time QTL. Epistatic pairs of QTL peaks were identified with the *qb.scantwo* function in R/qtlbim. Effects on DTF1 at the two SNPs closest to the QTL peaks were then extracted from the phenotypic values with the R/qtl function *effectplot*.

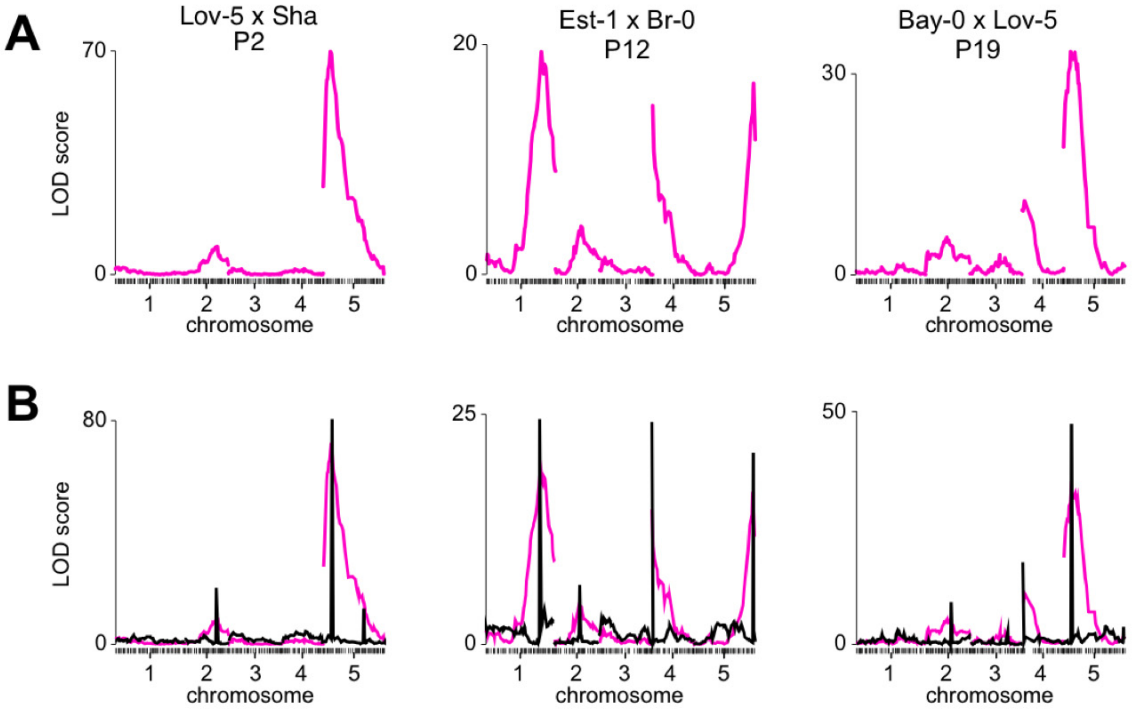

FIGURE S6.–Convergence of interval mapping and composite interval mapping. (A) Simple interval mapping results for P2 (Lov-5 x Sha), P12 (Est-1 x Br-0) and P19 (Bay-0 x Lov-5). (B) Composite interval mapping results for the same populations. Although LOD scores increase following CIM, the position of the QTL remains unchanged, as is, in most cases, the number of detected QTL.

TABLE S1

List of flowering time-related traits recorded in this study

Phenotype	Description
DTF1	Days until visible flower buds in the center of the rosette
DTF2	Days until inflorescence stem reached 1 cm in height
DTF3	Days until first open flower
RLN	Rosette Leaf Number
CLN	Cauline Leaf Number
TLN	Total Leaf Number: sum of RLN and CLN
LIR1	Leaf Initiation Rate (RLN/DTF1)

TABLE S2

Positions and confidence intervals of detected QTL peaks for DTF1

Population	Chr	Position	95% confidence interval	LOD score
P2	2	14,844,195	12,717,797-14,844,195	8.8
Lov-5 x Sha	5	3,162,852	3,162,852-3,619,476	69.8
P3 Bur-0 x Bay-0	1	26,099,650	24,810,967-26,357,422	7.6
	2	9,461,465	7,633,698-18,324,318	4.8
	3	20,547,090	15,522,173-21,142,865	6.4
	4	434,712	434,712-2,775,749	7.4
	5	21,901,746	17,959,456-24,757,037	5.7
P6 Van-0 x Bor-4	1	27,634,939	27,230,162-29,058,956	10.1
	3	11,107,344	10,358,588-14,244,642	3.4
	5	4,233,682	2,736,279-25,683,652	4.0
P7	4	434,712	434,712*	15.7
NFA-8 x Van-0	5	2,229,415	2,229,415-4,448,082	12.1
P8 Est-1 x RRS7	1	24,810,967	22,975,205-26,099,650	10.0
	4	10,607,774	8,585,617-17,031,668	4.1
	5	7,340,989	7,047,330-13,848,611	12.7
P9 Tsu-1 x RRS10	1	24,114,746	23,906,908-24,114,746	10.9
	4	434,712	434,712-5,643,991	5.9
	5	4,233,682	4,448,082-5,535,964	16.7
	5	25,612,289	24,757,037-25,899,673	37.8
P10 Bur-0 x Cvi-0	1	27,855,083	27,634,939-29,058,956	4.2
	4	7,724,867	3,002,169-10,089,916	14.1
	5	24,070,109	24,070,109*	24.5
P12 Est-1 x Br-0	1	24,114,746	23,906,908-26,099,650	19.4
	1	28,132,789		12.6
	2	11,537,081	10,556,376-13,659,835	4.2
	4	434,712	434,712*	14.7
	5	26,040,116	25,899,673-26,040,116	16.6
P15 Br-0 x C24	1	29,058,956	29,058,956*	24.4
	2	15,445,245	11,537,081-16,600,230	3.75
	5	3,162,852	1,917,139-5,010,563	9.3
P17 Cvi-0 x RRS7	1	12,686,038	11,838,780-13,207,971	4.8
	1	29,058,956	27,230,162-30,269,940	6.8
	2	17,124,023	17,124,023*	8.8
	4	13,960,078	11,320,394-18,060,948	5.2
	5	26,040,116	25,612,289-26,040,116	5.8
P19	2	9,461,465	8,225,326-12,019,213	5.6
Bay-0 x Lov-5	4	1,512,987	1,512,987*	11.0

	5	3,162,852	3,162,852-5,010,563	33.35
P20	4	208,650	208,650-1,512,987	10.3
Bor-4 x NFA-8	5	3,162,852	27,343-6,801,277	3.7
P35 Tamm-2 x Col-0	1	27,855,083	768,865-30,393,984	3.3
	3	13,495,379	10,358,588-18,532,958	3.7
	4	434,712	434,712-6,293,204	7.6
	5	4,233,682	3,619,476-6,055,546	19.8
	5	26,040,116	14,303,285-26,040,116	3.6
P66	1	29,333,952	24,810,967-29,333,952	6.7
Fei-0 x Col-0	5	26,040,116	1,166,716-26,040,116	3.1
P129 C24 x RRS10	1	29,333,952	29,333,952*	20.2
	2	11,537,081	8,561,080-17,729,906	4.2
	5	4,448,082	2,904,105-4,448,082	57.4
P145 Sha x Fei-0	1	29,333,952	27,230,162-30,269,940	4.3
	4	208,650	208,650-945,976	10.5
	5	1,603,469	271,377-23,272,788	4.5
P169	1	28,172,831	28,172,831*	49.4
Ts-1 x Tsu-1	5	25,683,652	24,757,037-25,683,652	17.2

*for very high-confidence QTL peaks, the 95% confidence interval is exactly the SNP with the highest LOD score.

TABLE S3

Positions and confidence intervals of detected QTL peaks for TLN

Population	Chr	Position (bp)	95% confidence interval	LOD score
P2 Lov-5 x Sha	1	4,519,429	3,779,036-5,506917	5.3
	2	11,193,105	7,400,522-19,006196	3.7
	5	2,229,415	2,229,415-3,619476	41.2
P3 Bur-0 x Bay-0	1	26,099,650	25,143,391-26,357,422	9.7
	3	20,547,090	16,629,399-22,221,736	4.9
	4	1,782,389	434,712-5,196,578	5.7
	5	24,757,037	3,858,361-25,683,652	6.6
P6 Van-0 x Bor-4	1	29,058,956	28,132,789-30,393,984	10.7
	2	9,461,465	8,561,080-11,537,081	8.8
	5	23,272,788	21,757,545-23,272,788	10.1
P7 NFA-8 x Van-0	1	24,810,967	24,810,967-25,520,382	6.8
	4	434,712	434,712*	30.2
	5	3,162,852	3,162,852-4,448,082	20.95
P8 Est-1 x RRS7	1	24,810,967	24,810,967-25,143,391	282
	4	14,957,828	14,957,828-17,325,108	14.5
	5	10,488,859	9,881,268-18,638,175	5.85
P9 Tsu-1 x RRS10	1	24,114,746	23,906,908-24,114,746	13.9
	4	434,712	208,650-4,169,509	4.0
	5	5,010,563	4,448,082-5,535,964	10.7
	5	25,612,289	24,757,037-25,612,289	37.2
P10 Bur-0 x Bay-0	1	29,058,956	27,634,939-30,065,751	5.8
	4	10,089,916	9,167,906-10,607,774	20.7
	5	24,070,109	24,070,109-24,757,037	29.5
P12 Est-1 x Br-0	1	24,111,746	24,114,746-27,855,083	21.8
	1	27,634,939	24,114,746-27,855,083	22.9
	2	12,019,213	10,556,376-12,717,797	8.0
	4	434,712	434,712*	26.3
	5	26,040,116	25,899,673-26,040,116	12.95
P15 Br-0 x C24	1	29,058,956	29,058,956*	39.2
	2	11,537,081	498,807-15,782,230	3.1
	5	1,917,139	1,917,139-3,162,852	19.9
P17 Cvi-0 x RRS7	1	29,058,956	28,548,488-29,058,956	11.4
	3	9,924,267	5,891,629-15,913,994	3.8
	4	15,863,233	11,320,394-17,538,469	18.7
	5	25,683,652	25,612,289-25683652	12.4
P19 Bay-0 x Lov-5	1	11,139,723	32,807-12,179,065	3.3
	2	9,461,465	2918,308-15,980,603	4.05

	4	434,712	434,712-1,512,987	11.4
	5	5,010,563	3,162,852-5,010,563	31.4
P20	4	208,650	208,650*	30.6
Bor-4 x NFA-8	5	5,535,964	3,162,852-8,427,379	8.1
	1	22,975,205	768,,865-30,393,984	3.7
	2	11,193,105	4,778,556-19,091,793	3.3
P35	3	13,495,379	13,495,379-17,211,862	5.5
Tamm-2 x Col-0	4	434,712	434,712*	11.3
	5	5,337,548	27,36,279-6,055,546	9.6
	5	26,040,116	25,612,289-26,040,116	7.6
P66	1	24,114,746	24,114,746-25,520,382	25.2
Fei-0 x Col-0	2	15,097,876	12,019,213-17,766,645	8.05
	5	26,040,116	26,040,116*	8.6
P129	1	29,333,952	29,333,952-30,065,751	10.0
C24 x RRS10	5	2,904,105	27,634,939-30,269,940	19.9
P145	1	29,333,952	28,172,831-30,269,940	5.7
Sha x Fei-0	4	208,650	208,650*	14.0
	5	1,603,469	1,603,469*	14.6
P169	1	28,172,831	27,634,939-28,172,831	58.55
Ts-1 x Tsu-1	5	25,683,652	25,683,652*	19.9

*for very high-confidence QTL peaks, the 95% confidence interval is exactly the SNP with the highest LOD score.

TABLE S4

Epistatic pairs between QTL detected by R/qtlBIM

Population	Chr	Position	Chr	Position	Variance
P2 (Lov-5 x Sha)	2	14,844,195	5	3,162,852	1.4
P2 (Lov-5 x Sha)	5	3,162,852	5	16,816,665	0.35
P7 (NFA-8 x Van-0)	4	434,712	5	2,229,415	2.5
P9 (Tsu-1 x RRS10)	4	434,712	5	4,233,682	0.85
P9 (Tsu-1 x RRS10)	1	24,114,746	5	25,612,289	1.5
P10 (Bur-0 x Cvi-0)	1	27,855,083	4	7,724,867	0.55
P12 (Est-1 x Br-0)	1	28,132,789	5	26,040,116	2.3
P15 (Br-0 x C24)	1	29,058,956	5	3,162,852	2
P20 (Bor-4 x NFA-8)	4	208,650	5	3,162,852	3.3
P35 (Tamm-2 x Col-0)	4	434,712	5	26,040,116	3
P129 (C24 x RRS10)	1	29,333,952	5	4,448,082	0.45
				Mean:	1.65%

TABLE S5

RIL Populations Characterized for Flowering Time QTL

Parent 1	Parent 2	Publication
Ler	Cvi	(ALONSO-BLANCO *et al.* 1998)
Ler	Col	(WEINIG *et al.* 2002)
Bay-0	Sha	(LOUDET *et al.* 2002)
Ler	Sha	(EL-LITHY *et al.* 2004)
Nd-1	Col	(WERNER *et al.* 2005)
Ler	An-1	(EL-LITHY *et al.* 2006)
Ler	Kas-2	(EL-LITHY *et al.* 2006)
Ler	Kondara	(EL-LITHY *et al.* 2006)
Blh-1	Col-0	(SIMON *et al.* 2008)
Bur-0	Col-0	(SIMON *et al.* 2008)
Ct-1	Col-0	(SIMON *et al.* 2008)
Cvi-0	Col-0	(SIMON *et al.* 2008)
Sha	Col-0	(SIMON *et al.* 2008)
Wt-5	Ct-1	(O'NEILL *et al.* 2008)
Sorbo	Gy-0	(O'NEILL *et al.* 2008)
Kondara	Br-0	(O'NEILL *et al.* 2008)
Cvi-0	Ag-0	(O'NEILL *et al.* 2008)
Ts-5	240#14	(O'NEILL *et al.* 2008)
Nok-3	Ga-0	(O'NEILL *et al.* 2008)

TABLE S6

Polymorphisms found in the *MAF2* gene

		nonsyn	nonsyn	syn
	Col-0	V	V	
	changed to	F	I	
QTL	position	25,999,656	25,999,773	26,002,211
	population			
no	Van-0 x Bor-4	-	-	-
no	NFA-8 x Van-0	NFA-8	-	--
no	Est-1 x RRS7	-	-	Est-1
no	Br-0 x C24	-	-	-
no	Bay-0 x Lov-5	-	-	-
no	Bor-4 x NFA-8	NFA-8	-	-
no	C24 x RRS10	RRS10	-	-
no	Sha x Fei-0	Fei-0	-	-
yes	Lov-5 x Sha	-	-	-
yes	Bur-0 x Bay-0	-	Bur-0	-
yes	Tsu-1 x RRS10	RRS10	-	-
yes	Bur-0 x Cvi-0	-	Bur-0	-
yes	Est-1 x Br-0	-	-	Est-1
yes	Cvi-0 x RRS7	-	-	-
yes	Tamm-2 x Col-0	-	-	-
yes	Fei-0 c Col-0	Fei-0	-	-
yes	Ts-1 x Tsu-1	-	-	-

- indicates when the two parental accessions share the same SNP.

TABLE S7

Polymorphisms found in the *FLC* gene

		syn	nonsyn	syn
	Col-0		Q	
	changed to		*	
QTL	position	3,175,629	3,174,836	3,173,806
	population			
no	Est-1 x RRS7	-	-	-
no	Bur-0 x Cvi-0	-	-	-
no	Est-1 x Br-0	-	-	-
no	Cvi-0 x RRS7	-	-	-
no	Fei-0 x Col-0	-	-	-
no	Ts-1 x Tsu-1	-	-	-
yes	Lov-5 x Sha	-	-	-
yes	Bur-0 x Bay-0	-	-	-
yes	Van-0 x Bor-4	-	Van-0	-
yes	NFA-8 x Van-0		Van-0	
yes	Tsu-1 x RRS10	RRS10	-	-
yes	Br-0 x C24	-	-	-
yes	Bay-0 x Lov-5	-	-	-
yes	Bor-4 x NFA-8	-	-	-
yes	Tamm-2 x Col-0	-	-	Tamm-2
yes	C24 x RRS10	RRS10	-	-
yes	Sha x Fei-0	-	-	-

- indicates when the two parental accessions share the same SNP.

TABLE S8

Polymorphisms found in the *FRIGIDA* gene

		nonsyn	syn	nonsyn	nonsyn	nonsyn
	Col-0	P		T	F	T
	changed to	T		M	I	I
QTL	position	269,059	269,088	269,162	269,188	269,237
	population					
no	Lov-5 x Sha	-	-	-	-	-
no	Van-0 x Bor-4	-	-	-	-	-
no	Est-1 x RRS7	-	-	-	-	-
no	Bur-0 x Cvi-0	Cvi-0	-	-	-	-
no	Br-0 x C24	-	-	-	-	-
no	Cvi-0 x RRS7	Cvi-0	-	-	-	-
no	Fei-0 x Col-0	-	-	-	-	-
no	C24 x RRS10	-	-	-	-	-
no	Ts-1 x Tsu-1	-	-	-	-	Ts-1
yes	Bur-0 x Bay-0	-	-	-	-	-
yes	NFA-8 x Van-0	-	-	NFA-8	-	-
yes	Tsu-1 x RRS10	-	-	-	-	-
yes	Est-1 x Br-0	-	-	-	-	-
yes	Bay-0 x Lov-5	-	-	-	-	-
yes	Bor-4 x NFA-8	-	-	NFA-8	-	-
yes	Tamm-2 x Col-0	-	-	-	Tamm-2	-
yes	Sha x Fei-0	-	-	-	-	-

nonsyn	nonsyn	nonsyn	nonsyn	nonsyn	syn
R	L	I	D	K	
C	I	M	E	*	
269,245	269,260	269,469	269,526	269,719	269,892
-	-	Lov-5	-	-	-
Bor-4	Van-0	-	Bor-4	-	-
-	RRS7	Est-1	-	-	-
Cvi-0	-	-	Cvi-0	Cvi-0	-
-	-	-	Br-0	-	-
Cvi-0	RRS7	-	Cvi-0	Cvi-0	-
-	-	Fei-0	-	-	-
-	-	C24	-	-	-
-	Tsu-1	-	-	-	-
-	Bay-0	-	-	-	-
-	Van-0	-	-	-	NFA-8
-	Tsu-1	Tsu-1	-	-	-
-	-	Est-1	Br-0	-	-
-	Bay-0	-	-	-	-
Bor-4	-	-	Bor-4	-	NFA-8
-	-	Tamm-2	-	-	-
-	-	Fei-0	-	-	-

- indicates when the two parental accessions share the same SNP.

SUPPORTING REFERENCES

ALONSO-BLANCO, C., S. E. EL-ASSAL, G. COUPLAND and M. KOORNNEEF, 1998 Analysis of natural allelic variation at flowering time loci in the Landsberg erecta and Cape Verde Islands ecotypes of Arabidopsis thaliana. Genetics **149:** 749-764.

BUCKLER, E. S., J. B. HOLLAND, P. J. BRADBURY, C. B. ACHARYA, P. J. BROWN *et al.*, 2009 The genetic architecture of maize flowering time. Science **325:** 714-718.

EL-LITHY, M. E., L. BENTSINK, C. J. HANHART, G. J. RUYS, D. ROVITO *et al.*, 2006 New Arabidopsis recombinant inbred line populations genotyped using SNPWave and their use for mapping flowering-time quantitative trait loci. Genetics **172:** 1867-1876.

EL-LITHY, M. E., E. J. CLERKX, G. J. RUYS, M. KOORNNEEF and D. VREUGDENHIL, 2004 Quantitative trait locus analysis of growth-related traits in a new *Arabidopsis* recombinant inbred population. Plant Physiol. **135:** 444-458.

LOUDET, O., S. CHAILLOU, C. CAMILLERI, D. BOUCHEZ and F. DANIEL-VEDELE, 2002 Bay-0 x Shahdara recombinant inbred line population: a powerful tool for the genetic dissection of complex traits in *Arabidopsis*. Theor. Appl. Genet. **104:** 1173-1184.

NORDBORG, M., T. T. HU, I. Y., J. JHAVERI, C. TOOMAJIAN *et al.*, 2005 The pattern of polymorphism in *Arabidopsis thaliana*. PLoS Biol. **3:** e196.

O'NEILL, C. M., C. MORGAN, J. KIRBY, H. TSCHOEP, P. X. DENG *et al.*, 2008 Six new recombinant inbred populations for the study of quantitative traits in *Arabidopsis* thaliana. Theor. Appl. Genet. **116:** 623-634.

SIMON, M., O. LOUDET, S. DURAND, A. BERARD, D. BRUNEL *et al.*, 2008 Quantitative trait loci mapping in five new large recombinant inbred line populations of Arabidopsis thaliana genotyped with consensus single-nucleotide polymorphism markers. Genetics **178:** 2253-2264.

WEINIG, C., M. C. UNGERER, L. A. DORN, N. C. KANE, Y. TOYONAGA *et al.*, 2002 Novel loci control variation in reproductive timing in *Arabidopsis thaliana* in natural environments. Genetics **162:** 1875-1884.

WERNER, J. D., J. O. BOREVITZ, N. WARTHMANN, G. T. TRAINER, J. R. ECKER *et al.*, 2005 Quantitative trait locus mapping and DNA array hybridization identify an *FLM* deletion as a cause for natural flowering-time variation. Proc. Natl. Acad. Sci. USA **102:** 2460-2465.